SYNTHESIS, CHARACTERIZATION, AND LIGHTING APPLICATIONS OF GROUP 11 METALLOPOLYMERS WITH TUNABLE PHOSPHORESCENCE

A THESIS

SUBMITTED IN PARTIAL FULFILLMENT OF THE REQUIREMENTS FOR THE DEGREE OF MASTER OF SCIENCE

IN THE GRADUATE SCHOOL OF THE

TEXAS WOMAN'S UNIVERSITY

COLLEGE OF ARTS AND SCIENCES

BY

MAHIR ALRASHDAN, B.S.

DENTON, TEXAS

DECEMBER 2009

TEXAS WOMAN'S UNIVERSITY

DENTON, TEXAS

August 21, 2009

To the Dean of the Graduate School:

I am submitting herewith a thesis written by Mahir Alrashdan entitled "The synthesis. characterization, and lighting application of group 11 metallopolymers with tunable phosphorescence." I have examined this thesis for form and content and recommend that it be accepted in partial fulfillment of the requirements for the degree of Master of Science with a major in Chemistry.

Manal Rawashdeh-Omary

Dr. Manal Omary, Major Professor

We have read this thesis and recommend its acceptance:

Manal Rawashdeh-Omary

Department Chair

Accepted: Jennifer Martin

Dean of the Graduate School

ACKNOWLEDGMENTS

Thanks foremost are due to God, the most merciful, and the compassionate, for all the blessings that He has given me. My special thanks go to Dr. Manal Omary, my MS dissertation advisor, for her guidance, tutelage, patience and support throughout this endeavor. Her wisdom, enthusiasm, and encouragement only add to the great scientific experience that Dr. Omary has. She is like a big sister to whom I will always be appreciative of her scientific advice and personal friendship. I would like to thank the Omary group members for their support and friendship. I also thank my advisory committee for their feedback and suggested corrections and improvements for the dissertation. Special thank goes to Dr. Mohammad Omary for his support and advice througout this thesis. I wish to thank all of Dr. Mohammad group for their help especially Gustavo Salazar and Roy MacDonald. Also special thanks to Prof. Khalil Alasali (Jordan University of Science and Technology) because of whom I pursued my graduate study. I would like to thank my colleague and good friend Priya vasabhaktula for her friendship, special thanks to Dr. Oussama elbjermi and his wife suha and lovely children Sarah and Yousef, but certainly not last, my deepest gratitude goes to my parents (Daifalla and Amina), my brothers and sisters along with their families, for their constant encouragement and ample compassionate support in my attainment of this goal to obtain a MS in chemistry.

ABSTRACT

MAHIR ALRASHDAN

SYNTHESIS, CHARACTERIZATION, AND LIGHTING APPLICATIONS OF GROUP 11 METALLOPOLYMERS WITH TUNABLE PHOSPHORESCENCE

DECEMBER 2009

This thesis with it 66 pp., 3 tables, 26 Figures and references is a study of group 11 monovalent metallopolymers. Three major chapters that involve synthetic strategies to obtain and enhance the phosphorescence of luminescent metallopolymer have been investigated. The first chapter includes an introduction to photoluminescence, luminescent group 11 monovalent complexes, metallopolymers and their application as light emitting diodes. The second chapter includes the photophysical properties of the gold (I) metallopolymers, which have been investigated and found to exhibit Au-centered tunable phosphorescence. The third chapter includes the photophysical properties of the silver (I) and copper(I) metallopolymer, which have been investigated as less-expensive alternatives to Au(I) analogues and found to exhibit metal-centered phosphorescence. The spectroscopic and materials properties of all metallopolymers are compared and contrasted versus the metal ion, ligands in the metal precursor.

TABLE OF CONTENTS

Page

LIST OF FIGURES

Figure Page

LIST OF TABLES

CHAPTER I

Introduction

This thesis is a study of the synthesis and spectroscopic features of group 11 based metallopolymers. Chapter one presents a literature review of the relevant topics. Section 1.1 describes the photoluminescence processes. Section 1.2 addresses the spectroscopy of small coordination compounds of group 11 monovalent ions (Au(I), Ag(I) and Cu(I)) in general. Section 1.3 is an overview of metallopolymers and their advantages in luminescent devices. Section 1.4 emphasizes on the role of group 11 metallopolymers in fabrication of polymer light emitting diodes (PLEDs). Finally section 1.5 discusses how this thesis attempts to address the approach used to synthesize the group 11 monovalent luminescent metallopolymers and possibly incorporate them into devices.

1.1 Introduction to Photoluminescence.

Photoluminescence is a radiative photophysical process that includes fluorescence and phosphorescence emissions of light, due to photophysical process whereby the molecule returns to its ground structure intact (as opposite to photochemistry where a permanent structural change takes place), Fluorescence results from a radiative transition between two electronic states of the same spin multiplicity[1-4], while phosphorescence occurs due to the radiative transition between two states of different spin multiplicity[1,5,6]. For a photophysical transition to occur, a discrete quantity of light (photon) of the appropriate wavelength and energy should be absorbed. This will cause the molecule to

gain an excess energy, and result in the formation of an energetically unstable state (electronic excited state) relative to the ground state of the molecule. The excited molecule may consequently undergo a chemical reaction, or just use its energy by a photophysical sequences of deactivations by non-radiative and radiative processes[7]. Figure1 represents a Jablonski diagram which illustrates all possible non-radiative and radiative routes of phototransition processes of typical organic molecular. The excited molecule can go in an internal conversion process that involves the dissipation of energy of the molecule to the surrounding in a nonraditive process.

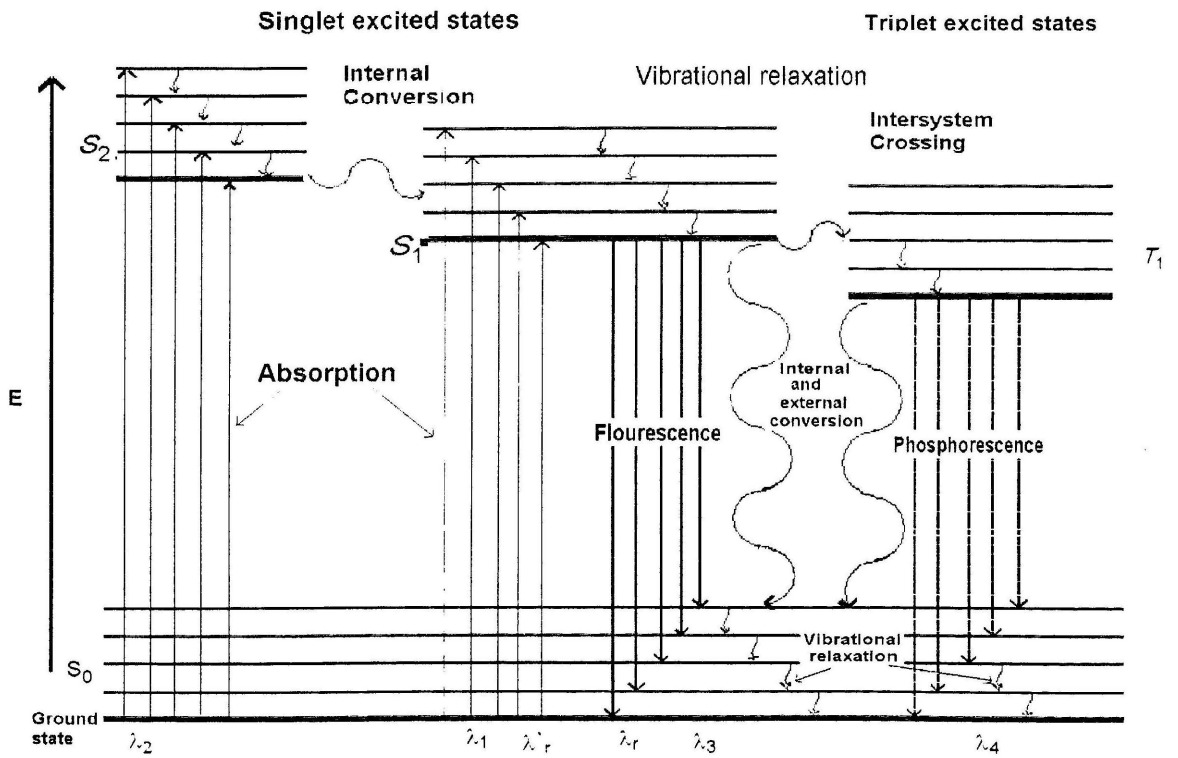

Figure 1. Partial energy level diagram for a photoluminescent system. It illustrates all possible non-radiative and radiative routes of phototransition processes of typical organic molecules.[8]

The radiative transitions that result are allowed, or forbidden, depending on whether they obey certain factors known as the selection rules. In general, the selection rules are governed by spin multiplicity; for example, the forbidden transition is relatively slow and is featured by its relatively long lifetime, which can continue for several seconds for typical organic molecules in a process called phosphorescence. Spin selection rules (by which phosphorescence is forbidden and fluorescence is allowed) can be violated in the presence of significant spin-orbit coupling as is observed for group 11 monovalent ions. A spin forbidden triplet to singlet transition is quite common in multiple classes of gold compounds and other heavy metal complexes that exhibit bright phosphorescence[7 9]. it can be dramatically accelerated for Au (I) heavy metal complexes[5] due to the large spin-orbit coupling in this very heavy molecule (ξ= 5100 cm^{-1}).

The efficiency of the luminescent transitions is measured by the quantum yield value (QY)[10,11], which is defined as the ratio of the emissive photons to excited ones[10](see Eq.1). The importance of this value is considered to be highly profound[12] because not only does it determine the relative brightness among different luminescent materials, but is also involved in calculating of quenching rate constants (k_q), energy transfer rate, and radiative and nonradiative rate constants (k_r and k_{nr}, respectively)[12]. This determination gives more comprehensive quantitative assessment of the photophysical behavior of a given luminescent material. The photoluminescence (PL) value can be influenced by several factors such as temperature, rigidity of the system, presence of water, molecular oxygen, transition metals and/or other quenchers or sensitizers [10,13] .When measuring the QY, one should take into consideration the inner

filter effect, the purity of the sample, complete solubility of liquid samples and uniformity of solid samples, polarization, scattering and finally the photostability of the luminescent compound[3,14], due to which erroneous and miscalculated values of the QY could be obtained. Equation 1 permits a qualitative interpretation of many of the structural and environmental factors that influence QY value (Φ).

$$\Phi = \frac{\text{number of photons emitted}}{\text{number of photons absorbed}} = \frac{k_r}{(k_r + k_{nr})} \qquad \text{Eq. 1}^{8}$$

1.2 Spectroscopic Properties of Group 11 Monovalent Ions.

Group 11 monovalent complexes have gained interest among researchers, due to their remarkable photochemistry and further application in the areas of photonics[15,16,17]. Group 11 transition metals have the tendency of forming metallophilic interactions between the metal ions generally named M—M interactions[18]. This has proven to be responsible for many electronic properties of group 11 monovalent ions compounds. These metal ions form a triplet excited state which can be attributed to the fact that their heavy atomic mass allows the spin-orbital coupling[19]. It is hard to determine whether the low energy electronic transitions in group 11 are due to M—M interaction or to low lying excited states of the metal especially for Au(I) and Cu(I). In either case, significant mixing with ligand orbitals usually takes place in such primarily metal-centered transition. Ligand –centered transition can also take place in some instances whereby the role of the metal is to provide spin-orbital coupling sensitization for the structured ligand phosphorescence [20-22].

The van der Waals radii values are used to determine whether M—M interactions exist in coordination compounds of group 11 monovalent ions. Table 1 lists the values of the van der Waals and covalent radii for the three metal ions of group 11. If the experimental M—M distance is lower than the value of summed van der Waals radii of the two metals, then it is an indication of the presence of M—M interaction, as rule of thumb. However, it has often been suggested that these radii are not strict requirements for the presenc e of metall ophilic interaction[23,24]. In general, intermolecular distances between M^I centers up to 3.6-3.8 Å may qualify as metallophilic interactions in term of a lower limit. While such long distances may not significantly influence the absorption energies, they can cause significant red shifts in the phosphorescent excited state on which excimeric bonding leads to shrinking of the ground state M—M distances[23,25,26].

Table 1.

Values of van der Waals r_{vdw} and covalent r_{cov} radii of group 11 M^I ions [27].

Element	r_{vdw} [16], Å	r_{cov} [22], Å
Cu	1.4	1.11
Ag	1.7	1.34
Au	1.7	1.25

The geometry of group 11 monovalent complexes is considerably profound in their photophysical properties. For example, Au(I) complexes most commonly exist as linear $Au(I)L_2$ (L = ligand) species; however $Au(I)L_3$ and $Au(I)L_4$ species are also known [28], the photoluminescence properties of these species differ from one coordination mode to

another. For example, $Au(I)L_2$ complexes display luminescence only in the presence of Au...Au (aurophilic) interactions[29,30], while $Au(I)L_3$ complexes exhibit luminescence with or without Au...Au interactions[30].

Rawashdeh-Omary and coworkers[23,31,32] illustrated that varying the metal in cyclic trinuclear complexes of Cu(I) , Ag(I) and Au(I) led to distinct variation in the solid state stacking and photophysical properties of those complexes. Some of them show remarkable photoluminescence tuning across the entire visible region; this tuning can be caused by exposure to a volatile organic solvent, varying the temperature, medium rigidity, concentration and/or excitation wavelength. For example, the$\{[3,5\text{-}(CF_3)_2Pz]Cu\}_3$[32] complex exhibits bright orange luminescence at room temperature in solid state. The crystal structure of the complex reveals two types of M—M distances, namely inter- and intra-molecular averaging 3.232 and 3.886 Å, respectively, and infinite zigzag chains of copper trimer due to the weak intermolecular interaction. Only the long intermolecular interaction between the copper trimer units is responsible for the luminescence activity despite the van der Waals summed radii indicating metal centered (^{3}MC) excimeric triplet state, as initially hypothesized based on spectroscopic data by Rawashdeh-Omary et al[33,34] and then later substantiated both computationally[35] and experimentally[36] via excited state crystallography. The complex $[Au_3(CH_3N{=}COCH_3)_3]$, on other hand, exhibits low-energy yellow luminescence that can be exhibited upon solvent contact without light in previously irradiated samples (called "solvo luminescence")[37,38]. This phosphorescence is due to intermolecular Au—Au distance close in value to the van der Waals distance in oligomers and extended stacks [37]. In

another example, Dias et al[39 4 0-42] reported several trinuclear silver(I) complexes of fluorinated pyrazolate compounds such as $\{[3\text{-}(CF_3)Pz]Ag\}_3$, $\{[3\text{-}(CF_3),5\text{-}(CH_3)Pz]Ag\}_3$, $\{[3\text{-}(CF_3),5\text{-}(Ph)Pz]Ag\}_3$, $\{[3\text{-}(CF_3),5\text{-}$ (But)Pz]$Ag\}_3$, and $\{[3\text{-}(C_3F_7),5\text{-}(But)Pz]Ag\}_3$. All of these complexes, crystals show argentophilic intermolecular interaction between the sliver atoms with an average distance of 3.390A. This distance was slightly longer than the van der Waals distances which seem to be influenced by the steric repulsions between the pyrazolyl ring substituents.

The Lewis acid base chemistry of these complexes is also "interesting" since it has an effect on their photophysical properties and solid state stacking[22,31,43-47]causing the tunable emission across the visible region. For example, facial interface of $\{[3,5\text{-}(CF_3)_2Pz]Ag\}_3$ complex with naphthalene led to the formation of the adduct Ag-naphthalene, which exhibits phosphorescence corresponding to T_1 monomer emission of naphthalene. Solid samples of this adduct exhibit bright-green phosphorescence at room temperature with an 830 μs lifetime while cooling to cryogenic temperatures shows increases in the intensity, lifetime, and vibronic resolution. The crystal structure of the adduct reveals an Ag- naphthalene distance of 3.00 Å, which is very close to the Ag-C van der Walls summed radii (3.42 Å). The relatively short phosphorescence lifetime of the adduct than the naphthalene alone, is caused by external heavy-atom effect of silver atoms. In another example, the gold trimer $[Au_3$ ((p-tolyl)N = C(OEt))$_3]$ with Lewis bases like $C_{10}F_8$ leads to the formation of π Lewis acid- base stacking of long-chain structures[48]. The Au—Au distance in the gold-adduct was longer than the gold trimer, alone (3.5 Å versus 3.25 Å, respectively). The resulting phosphorescent emission at room

temperature was assigned to T_1 state monomer emission of the $C_{10}F_8$. The reduction of lifetime and the emission energy of naphthalene phosphorescence is caused by the external heavy atom effect of the gold atoms.

1.3 Overview of Metallopolymers and their Advantages.

The first attempt to use polymer in light emitting devices was initiated by the discovery of the first luminescent polymer in 1989 at Cambridge University [49]. However, the efficiency of the initial devices was very low[50]. Since then metallopolymers have attracted the interest of many researchers because they combine the physical and mechanical characteristics of polymers with the electrical and optical properties of transition metal complexes[51]. For example, using phosphorescent metal complexes instead of organic fluorophores in organic light emitting diodes (OLEDs)[52-54] has revolutionized that technology so the hope is that a transformational change upon using phosphorescent metallopolymers instead of fluorescent polymer in PLEDs. Particularly, the potential use of these materials in light-emitting diodes, photovoltaic cells, and other optoelectronic devices has motivated the development of synthesis of metallopolymer materials with unique properties[55]. The electronic characteristics of these materials are primarily controlled by the nature of the molecular conjugation, but intermolecular interactions also exert a significant influence on the macroscopic material properties[53].

The typical methods of synthesizing metallopolymers was by using a doped polymer with luminophorous transition metals[49,56]. Recently, a new development has been introduced to the field by coupling transition metal complexes to backbone of

polymers to give hybrid materials in which the properties of the metal complex may be joined to those of the conjugated polymers[57]. This high charge carrier mobility of the polymer may be coordinated with emitting metal groups. This can result in enhanced photophysical properties and superior device performance[58].

Metallopolymers have a number of advantages over small molecules in the fabrication of electroluminescent devices. For instance, they are mechanically flexible, and can be easily fabricated by techniques such as ink-jet printing versus sublimation methods used for fabrication of OLEDs, where a layer of small molecule emitters have to be vapor deposited onto devices at high temperatures. This can result in undesirable decomposition of the materials or crystallization problems. Furthermore, the color emitted from the polymeric materials can be readily customized by modifying the chemical structure, and this offers a distinct advantage over the use of traditional inorganic semiconductors.

1.4 Polymer Light Emitting Diodes.

The superior performance of Polymer Light Emitting Diodes (PLEDs) in terms of contrast, thinness, brightness, low power consumption, response speed, and viewing angle has been attracting scientist's attention in recent years. The technology is very energy efficient and lends itself to the creation of ultra-thin lighting displays that will operate at lower voltages. They have simpler device structures making it easier to fabricate by sample methods like room temperature processing with inkjet printing or spin coating versus high-vacuum

and high-temperature sublimation methods use for OLEDs. In addition, they have better performance in aspect of both charge transport and charge injection. Their technology is set to transform the display industry with its superior imaging performance[15,17,59], compact and lightweight properties[60]. It looks set to replace liquid crystal displays (LCDs) and cathode ray tubes (CRTs) in many existing applications. Figure 2 is an illustration of the basic structure of a PLED device which consists of several layers, each performing a specific function such as charge injection, charge transport and emissive light layer.

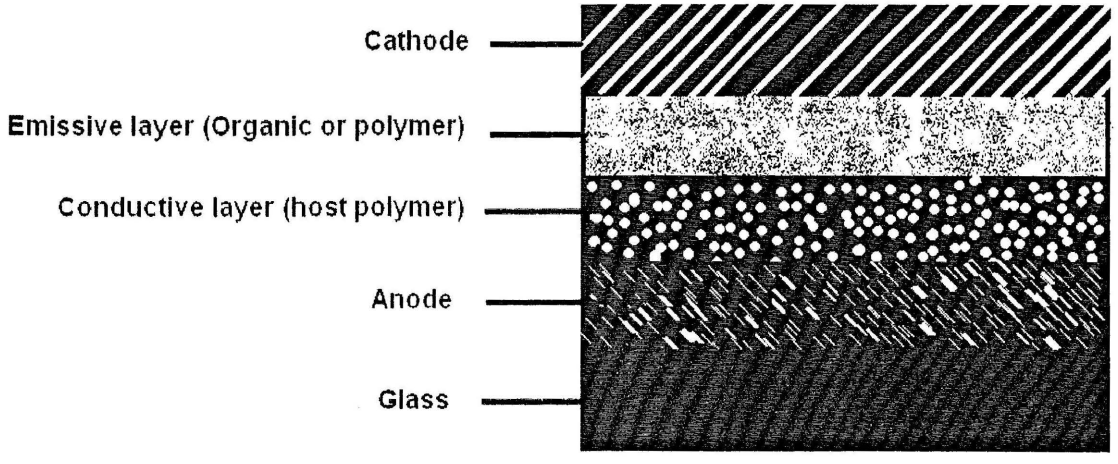

Figure 2. Basic Structure of PLEDs devices. Layers from top to bottom Cathode, Emissive Layer, Conductive Layer, Anode and Substrate [58].

Existing PLEDs often make use of electronically luminescent polymers which have inherent fluorescence. Typical organic materials have the non-luminescent triplet state. The presence of metal complexes (due to a strong spin orbit coupling) can display

a rapid intersystem crossing from lowest excited singlet state to lowest triplet state which often has a significantly short phosphorescence lifetime. Thus, we can observe the formation of excited singlet and triplet states thus resulting in luminescence [55,61].

A typical PLED consists of a thin layer of an undoped fluorescent conjugated polymer sandwiched between two electrodes on top of a glass substrate. The polymer is spin coated on top of a patterned indium-tin-oxide(ITO)bottom electrode which forms the anode and an evaporated Ca\Al metals layer is used as a cathode[62]. Appreciable efficiencies have been obtained by using transition metal complexes as emissive species. In hydrocarbon materials, the excited triplet states are typically nonemissive due the spin-forbidden nature of $T_1 \leftrightarrow S_0$ transitions, thereby limiting the internal electroluminescence efficiency to a maximum of 25%[63,64]. In principle, this major drawback can be overcome by significant spin-orbit coupling due to a heavy atom. Applying transition-metal complexes and organic luminophores into solid-state OLED devices has become an exciting field in recent years[65-67]. OLED designs are typically based on small molecules, like polycyclic aromatic hydrocarbons, or some polymers. The advantage of phosphorescent light-emitting materials is that they harness emission from both the singlet and triplet excited states generated via electroluminescence so it is possible to achieve OLEDs with 100% internal quantum efficiency whereas in fluorescent material there is a four-fold loss in the efficiency if photoluminescence efficiency was the same as that of the a phosphorescent molecule.[17,52,68].

1.5 The Rationale of This Thesis.

Throughout the duration of this research, we have made an effort to synthesize and characterize strongly luminescent metallopolymers for the goal of use in PLEDs or other optoelectronic applications. The presence of a transition metal will activate the triplet state. Thu s, instead of physical doping, we will focus on coordinating the metal to polymer to activate the triplet state and increase efficiency. Our strategy mainly focuses on coordination of σ donor polymer to σ accepter metal complex which may lead to novel class of phosphorescent metallopolymers. By altering the ligands, the metal and the polymer, we will be able to control their electronic and photophysical properties. In this thesis, we have tried coordinating a polymer like Poly(4-vinylpyridene) to various metal complexes with various ligands to obtain the new phosphorescent metallopolymers. A direct σ-coordination to a heavy metal takes place for suitable polymer of heterocyclic aromatic chromospheres . as they can undergo direct bonding to metal though the available lone pair on the N atoms. The resulting phosphorescent metallopolymers may have the interesting spectral properties of the small metal complexes mentioned earlier in section 1.2, along with the desirable photophysical and material properties of the polymer.

CHAPTER II

THE SYNTHESIS, CHARACTERIZATION, AND SPECTROSCOPIC MEASUREMENTS OF MONOVALENT GOLD (I) METALLOPOLYMERS

Direct coordination of gold (I) moieties to a σ donating polymer leads to a new class of monovalent gold(I) metallopolymers with fascinating photophysical properties, attributed in part to the ability of gold to form aurophilic bonding. The following chapter discusses the synthesis and the photophysical characterization of this new class of monovalent gold(I) metallopolymers. Section 2.1 covers in detail the synthetic methods of the gold(I) metallopolymers. Section 2.2 contents a description of the instruments used to characterize and collect the photophysical spectra of the gold(I) metallopolymers and present the chemical and materials used in the synthesis. Section 2.3 discusses the spectroscopic measurements obtained for the gold(I) metallopolymers in terms of emission, excitation, lifetime and QY for some of gold(I) metallopolymers. Finally section 2.4 summarizes the main conclusions and the prospective future directions about this project.

2.1 Synthesis

2.1.1 Synthesis of ClAuTHT

$$Au + HCl\backslash HNO_3 \longrightarrow HAuCl_4$$

$$HAuCl_4 + THT \longrightarrow ClAuTHT$$

With slight mollification to literature methods[69-71],12 ml of aqua regia (9 ml of HCl and 3 ml of HNO_3) was added to 1.8 g of gold metal and stirred until complete dissolving . While the temperature was maintained at 70°C, four measured additions of 1 mL of concentrated HCl were added every 30 min. After 2 h the solution was cooled to room temperature by addition of 50 mL mixture of 20 ml of ethanol and 30 ml of water. Four ml of tetrahydrothiophene was added to the solution and stirred for 30 min. The color change from golden yellow to orange solution was followed by the formation of white precipitate. The reaction mixture was filtered and washed with 30 ml of cold methanol and 30 ml of cold diethylether. It was finally dried by reduced pressure for 2 hours, A white crystalline solid was collected (90% yield) . The product was kept in the refrigerator and stored in a dark place. This gave us a white solid (yield 92 %) mp 60°C.

2.1.2 Synthesis of PVP AuCl.

$$ClAuTHT + PVP \longrightarrow PVPAuCl$$

PVP AuCl was prepared by reacting ClAuTHT with a corresponding stoichiometric ratio with PVP in dichloromethane at room temperature. The reaction occurs instantly and as clearly evidenced by the formation of a white precipitate and the

appearance of a bright green-blue luminescent product upon mixing the non-luminescent starting materials .The product was filtered and washed with dichloromethane to remove any unreacted PVP . FT-IR (KBr pellet): ν = 1615 cm^{-1} (C=N), ν = 3040 cm^{-1} (C=C-H aromatic). The gold content in the metallopolymer was determined via thermal gravimetric analyses (TGA). Thus, gold content was found to be 53% which corresponds to 91% of PVP occupied.

2.1.3 Synthesis. Of [Au(C_6F_5)PVP] Metallopolymer.

$Au(C_6F_5)THT + PVP \longrightarrow Au(C_6F_5)PVP$

[$Au(C_6F_5)THT$] was prepared according to literature method[72].PVP((0.046 g, 0.442 mmol)) was added to a solution of [$Au(C_6F_5)THT$] (0.200 g, 0.442 mmol) in dichloromethane (20 mL). The reaction occurs instantly and as clearly evidenced by the formation of a white precipitate. The reaction mixture was stirred for 2 h and evaporated to dryness under vacuum. Addition of 20 mL of diethylether followed by filtration led to a white solid (yield 59 %). Gold analysis (% wt): 35.55 %, that corresponds to 84% of occupied positions in the polymer. 1H NMR (400 MHz, d6- DMSO), δ 1.48 (bs, 2H, -CH_2 -), 6.97 (bs, H3, H5 Py ring) and 8 37 ppm (bs, H2, H6, Py ring) FT-IR (Nujol mulls): ν = 1615 cm^{-1} (C=N), ν = 1504, 955, 806 cm^{-1} (Au-C_6F_5).

2.1.4 Synthesis. Of [Au(C_6Cl_5)PVP] Metallopolymer .

$Au(C_6Cl_5)THT + PVP \longrightarrow Au(C_6Cl_5)PVP$

[$Au(C_6Cl_5)THT$] was prep ared according to literature method[72]. PVP(0.052 g, 0.493 mmol) was added to a solution of [$Au(C_6F_5)THT$] (0.263 g, 0.493 mmol) in dichloromethane (20 mL). The reaction occurs instantly and as clearly evidenced by the formation of a white precipitate. The reaction mixture was stirred for 2 h and evaporated to dryness under vacuum. Addition of 20 mL of diethylether followed by filtration led to a white solid (yield 60 %). Gold analysis (% wt): 29.8 % that corresponds to 83% of occupied positions in the polymer. FT-IR (Nujol mulls): ν = 1614 cm^{-1} (C=N), ν = 829, 630 cm^{-1} ($Au\text{-}C_6F_5$).

2.1.5 Synthesis of $C_6H_5CCAuTHT$.

C_6H_5CCH + nBuLi ⟶ C_6H_5CCLi + n Butane

C_6H_5CCLi + ClAuTHT ⟶ $C_6H_5CCAuTHT$ + LiCl

At -40° C (dry ice/acetonitrile), 0.66 mL of n-BuLi was added drop wise (1.05 mmol,1.6 M in hexanes) to 0.100 mL solution of phenylacetylene (1.05 mmol Mw't 102.14 g/mol d .93g/ml) in 5 ml of dry THF to Schlenk flask. Then stirred for 2 hours, then 0.336 g of ClAuTHT (1.05 mmol , Mw't 320g / mol) was added to the flask under positive pressure and then stirred for another 2 hours at -40° C, and 1 hour at RT .We observed the change in color from a colorless to a yellow colored solution. The solvent then removed under reduced pressure. A yellow solid with orange luminescence was obtained. The solid was washed with methanol and dried under vacuum for 2 hours, kept in refrigerator, mp was 80°C (deco). 1H NMR (500 MHz, d6- Acetone), δ 2.10 (bs, 2H, -

CH2 -), 3.20 (bs 2H, S-CH2-), 7.2-7.4 (Py ring). FT-IR (KBr pellet): ν = 1615 cm^{-1} (C=N), ν = 3040 cm^{-1} (C=C-H aromatic). Gold analysis (% wt): 64.0 %.

2.3.6 Synthesis of Metallopolymer C_6H_5CC-Au-PVP.

Method A

$C_6H_5CCAuTHT$ + PVP ⟶ C_6H_5CC-Au-PVP + THT

Metallopolymer [C_6H_5CC-Au-PVP] was prepared by reacting the stoichiometric molar ratio of $C_6H_5CCAuTHT$ with PVP (MW = 60,000 as obtained from Aldrich) in dichloromethane at room temperature. The reaction was stirred for 1 hour. The solid was filtered and washed with DCM to obtain a pale yellow solid (mp 120°C).

Method B

C_6H_5CCH + nBuLi ⟶ C_6H_5CCLi + n Butane

C_6H_5CCLi + PVPAuCl ⟶ $C_6H_5CCAuPVP$ + LiCl

Metallopolymer [C_6H_5CC-Au-PVP] was prepared by addition of stoichiometric mass of C_6H_5CCLi (see synthesis of $C_6H_5CCAuTHT$) to ClAuPVP in THF at -40C .The reaction allowed to stir for 1 hour. After filtering, the solid was washed with DCM to obtain a pale yellow solid mp of 120°C. FT-IR (KBr pellet): ν = 1615 cm^{-1} (C=N), ν = 3040 cm^{-1} (C=C-H aromatic), ν = 2950 cm^{-1} (C-C-H alkanes). Gold analysis (% wt): 64.0 %. The gold content in the metallopolymer was determined via thermal gravimetric analyses

(TGA). Thus, gold content was found to be 38.5% that corresponds to 78.7% of PVP occupied.

2.1.7 Synthesis of C_6F_5CCAu-THT.

C_6F_5CCH + nBuLi ⟶ C_6F_5CCLi + n Butane

C_6F_5CCLi + ClAuTHT ⟶ $C_6F_5CCAuTHT$ + LiCl

At -40° C (dry ice/acetonitrile) 0.320 mL of n-BuLi was added drop wise (5.10 X 10^{-4} mmol,1.6 M in hexanes) to 0.100 mL solution of pentafluorophenylacetylene (5.10 X 10^{-4} mmol Mw't 102.14 g/mol d .93g/ml) in 5 ml of dry THF to Schlenk flask and stirred for 2 hours. Then 5.10 X 10^{-4} was added to the flask under positive pressure and stirred for another 2 hours at -40° C, and 1 hour at RT. We observed the change from a colorless solution to a yellow colored solution. The solvent then removed under reduced pressure. A yellow solid with green luminescence was obtained. The solid was washed with methanol and dried under vacuum for 2 hours, kept in refrigerator, mp was 82°C (deco). 1H NMR (500 MHz, d6- Acetone), δ 2.10 (bs, 2H, -CH_2 -), 2.90 (bs 2H, S-CH_2-). FT-IR (KBr pellet): ν = 1610 cm-1 (C=N) ν = 2950 cm-1 (C=C-H alkane). Gold analysis (% wt): 27.0 %.

2.1.8 Synthesis of the Metallopolymer C_6F_5CCAu-PVP.

$C_6F_5CCAuTHT$ + PVP ⟶ C_6F_5CC-Au-PVP + THT

Metallopolymer [C_6F_5CCAu-PVP] was prepared by reacting the stoichiometric amount of $C_6F_5CCAuTHT$ with PVP (MW = 60,000 as obtained from Aldrich) in

dichloromethane at room temperature. The reaction allowed to stir for 1 hour. After filtering, the solid was washed with methanol to obtain a pale-yellow solid (mp 105°C), FT-IR (KBr pellet): ν = 1610 cm-1 (C=N) ν = 2950 cm-1 C-H Alkanes). Gold analysis (% wt): 38.4 %.

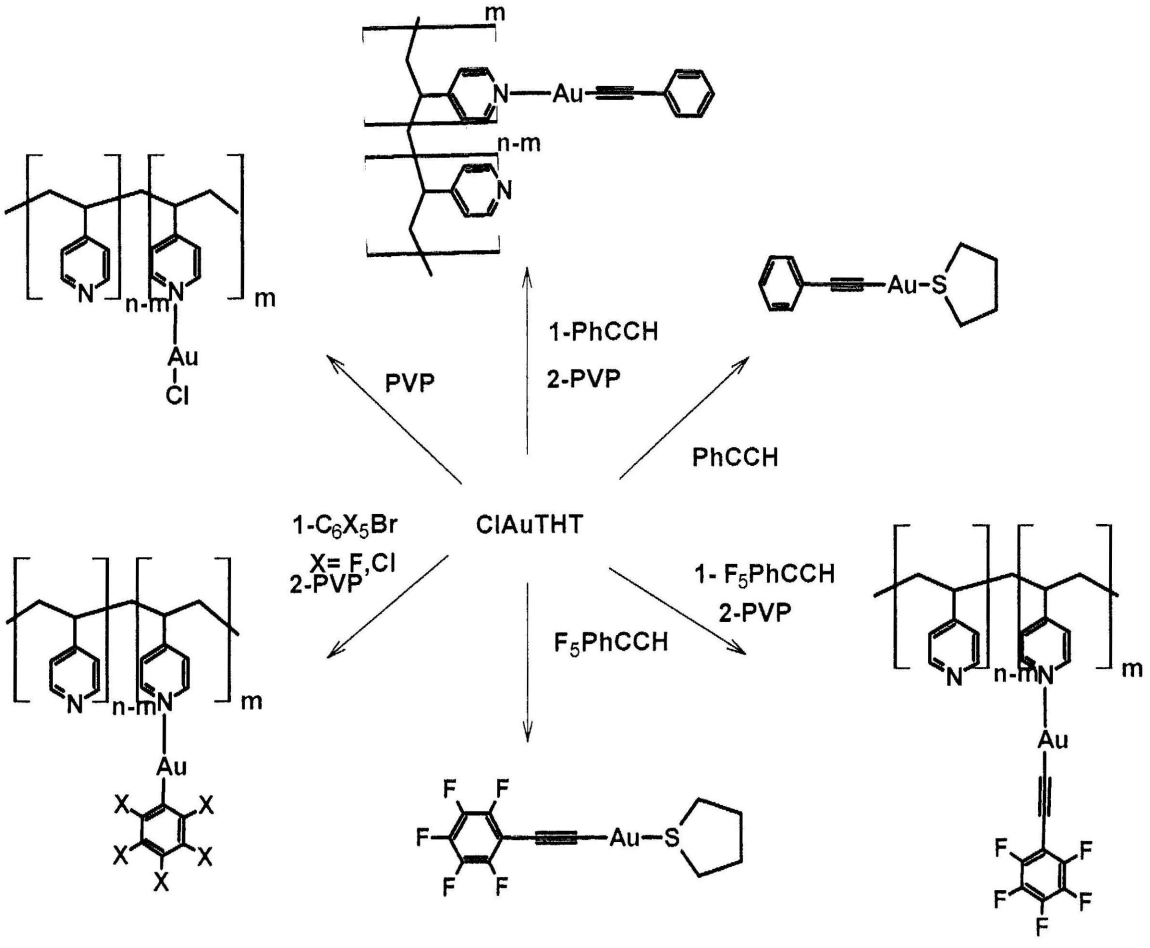

Figure 3. Illustration of synthesis routes of Gold (I) Metallopolymers

2.2 Instrumentation\ Chemicals and Materials

Steady-state photoluminescence spectra were acquired with a PTI QuantaMaster Model QM-3/2006SE scanning spectrofluorometer equipped with a 75-watt xenon lamp, emission and excitation monochromators, excitation correction unit, and a PMT detector. The emission spectra were corrected for the detector wavelength-dependent response. The excitation spectra were also corrected for the wavelength-dependent lamp intensity. Temperature-dependent studies were acquired with an Oxford optical cryostat using liquid nitrogen as a coolant. Lifetime data were acquired using a high speed pulsed xenon lamp source interfaced to the PTI instrument along with an autocalibrated "QuadraScopic" monochromator for excitation wavelength selection. Direct quantum yield measurements were performed for solid samples at an ambient temperature with an integrating sphere from LabSphere that is interfaced to the PTI instrument. To verify the reliability and accuracy of our techniques, we determined the direct quantum yield of quinine sulfate solution using this setup and attained the correct value of 0.53. The temperature-dependent quantum yields were determined from the relative peak areas of the emission bands at different temperatures at the same wavelengths used in the direct quantum yield measurements at ambient temperature. The luminescence titrations data were recorded with a Jobin-Yvon Horiba Fluorolog 3-22 Tau-3 spectrofluorometer, all other photophysical data were generated with the aforementioned PTI systems. Absorption spectra were acquired with a Perkin-Elmer Lambda 900 double beam and UV/VIS/NIR detector. The ^{1}HNMR was carried out on a Varian Mercury 500MHz NMR spectrometer. The chemical shift expressed as ξ values in parts per million from

tetramethylsilane as an internal standard. Melting points were determined on Mel-Tem capillary melting point apparatus. Infrared spectra were determined with a Nicolet 380 FT infrared spectrometer. Thermal gravimetric analysis (TGA) was determined by TA Q50 TGA, equipped with high sensitivity balance, Integrated Mass Flow Controllers and Integrated Mass Flow Controllers.

HPLC grade acetone, acetonitrile, tetrahydrofuran (THF), dichloromethane (DCM), methanol, toluene and benzene were purchased from Aldrich, and used after drying with conventional methods. phenylacetylene (C_6H_5CCH), n-butyllithium (1.6M in hexane), hydrochloric acid 37% , nitric acid 65%, tetrahydrothiophene (THT) and poly-(4-vinylpyridene) (PVP) (AMW =60,000) were purchased from Sigma Aldrich and used as is. Pentafluorophenylacetylene (C_6F_5CCH) was purchased from Paragos-Germany; high purity gold coins were purchased from Nasr Jewelry, Denton, TX.

All reactions were carried out by Schlenk technique under inert atmospheric conditions unless indicated otherwise.

2.3 Results and Discussion

We will start this discussion with the metallopolymer PVP-Au^{I}Cl since chloride ion is the simplest and the hardest ligand of all of the ligands we have used in this chapter. The halide Cl^- has a relatively small size compared to the other ligands used and it is considered a good π donor, leading to a possible transition as ligand to metal charge transfer (LMCT) upon binding to gold. The PVP-Au^{I}Cl metallopolymer is formed from mixing equal molar ratios of PVP and THTAuCl. It exhibited bright blue photoluminescence (PL) in the solid state at room temperature and 77 K. Temperature-dependent PL and PL excitation (PLE) spectra and lifetimes are shown in Figure 4. In the spectra, four emission maxima with λ_{em}=480, 500, 520 and 540 nm and two excitation maxima 330 and 370 nm at 77 K were observed. At RT one red shifted excitation band at 375 nm and two emission bands at 500 and 515 nm ware observed. Also, the 9.7 μs emission lifetime at 77 K dropped to 7.8 μs at room temperature (RT), indicating only minor increase in the nonradiative decay constant and thus very high phosphorescence quantum yield at RT. These data reveal remarkable sensitivity of the luminescence energies and intensities to both excitation wavelength and temperature. The emission can be fine-tuned between four emission maxima by varying λ_{exc} especially at cryogenic temperature. The tunable PL of the PVP-Au-Cl lie in the range of 60 nm at 77 K, that is from blue emission (λ_{em}=450 nm) to green emission (λ_{em}=570 nm). At room temperature, less resolvable peaks in the PL ware observed as the peaks coalesce into one broad peak and become less dependent on the excitation energy. On the other hand, 1:10 gold to

polymer molar ratio has also been synthesized to study the effect of the gold content on the photoluminescence and solubility properties. Figure 5 represents the PL and PLE of the metallopolymer PVP-Au^{I}Cl with 1:10 molar ratio. The bright blue emission of the metallopolymer using this ratio gives similar photophysical properties to that stoichiometric ratio of 1:1. It showed analogous spectral profile with tunable bright blue triplet state metal centered photoluminescence with a lifetime of 9.8 μs and 7.9 μs at 77 k and room temperature, respectively. Although the 1:10 molar ratio were strongly luminance which reduce the cost of synthesis, reducing the metal ratio led to low effect in the solubility property.

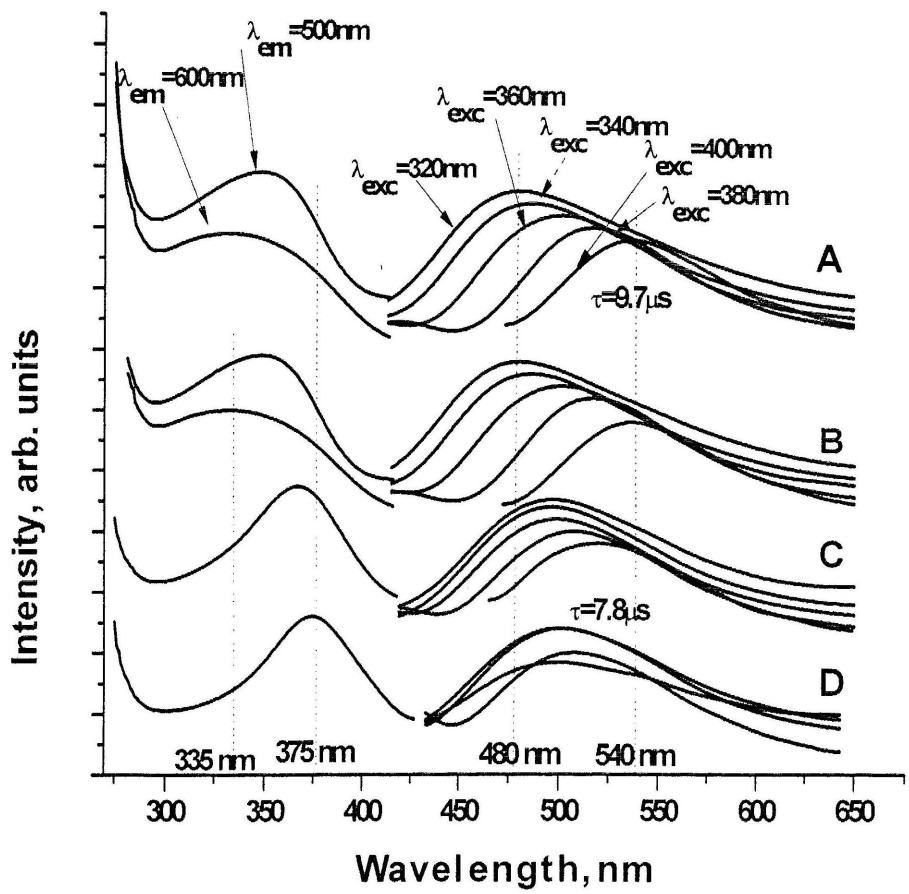

Figure 4. Solid state photoluminescence excitation (left) and emission (right) spectra at (A) 77K (B) 150K (C) 230K and (D) 298K of PVP-Au^{I}-Cl in ratio of 1:1. The labeled spectra show the emission is red shifted upon varying excitation (320, 340, 360, 380, and 400 nm respectively). The dotted lines represent the min and max peaks maxima for both excitation and emission spectra.

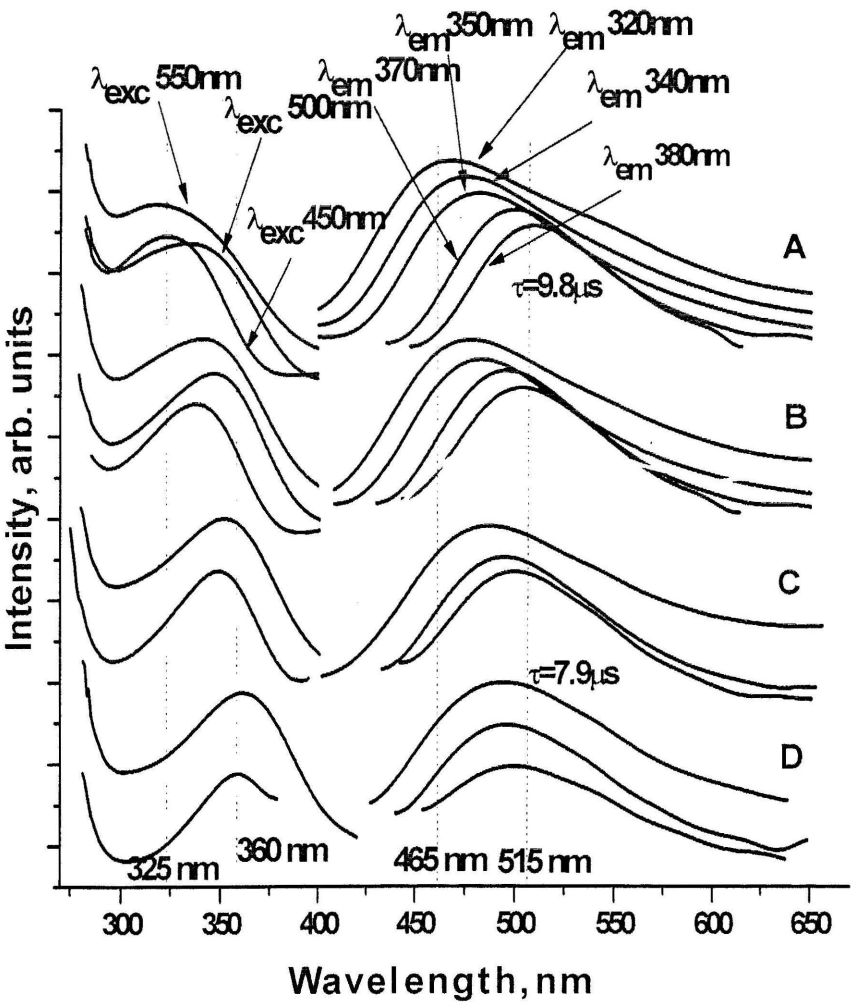

Figure 5. Solid state photoluminescence excitation (left) and emission (right) spectra at (A) 77K (B) 150 K (C) 230K and (D) 298K of PVP-$Au^{I}Cl$ in ratio of 10:1. The labeled spectra show the emission is red shifted upon varying excitation (320, 340, 350, 370, and 380 nm respectively). The dotted lines represent the min and max peaks maxima for both excitation and emission spectra.

We attribute this emission to aurophilic interaction (Au^{I}----Au^{I}), based on the literature reviews for linear two coordinate complexes of Au(I) system[73]. Gold-gold interactions can be intrachain or interchain interaction within the metallopolymer. Figure 6. Illustrates of the possibilities in which we expect multiple site interactions to occur

with difference in Au^{I}----Au^{I} distance. This leads to the corresponding temperature dependent excitation and emission obtained for these systems, as the different site interactions should have different excitation energies. The increase in temperature led to higher k_{nr} value leading to the different emission states to be quenched or peak broading.

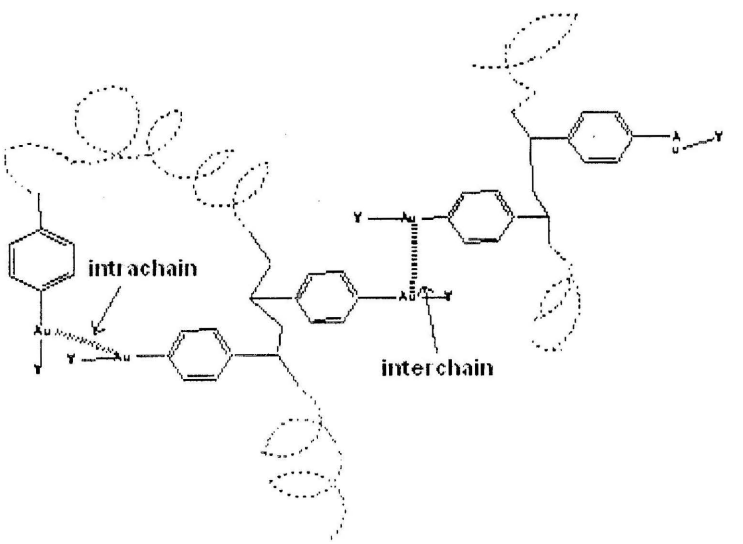

Figure 6. General suggested structural model shows interchain and intrachain aurophilic interaction.

Figure 7 shows the solid state diffuse reflectance of both the polymer PVP and the metallopolymer PVPAuCl. The PVP diffuse reflectance spectra showed absorption maximum at 255 nm. This suggests л to л* transition which is a feature of conjugated aromatic organic compounds. Upon coordination of the $ClAu^{I}$ moiety to the PVP polymer, this absorption maximum shifted to 265 nm, but the overall spectra look very similar, indicating that PVP is the main chromophore for possible light absorption (Figure 7).

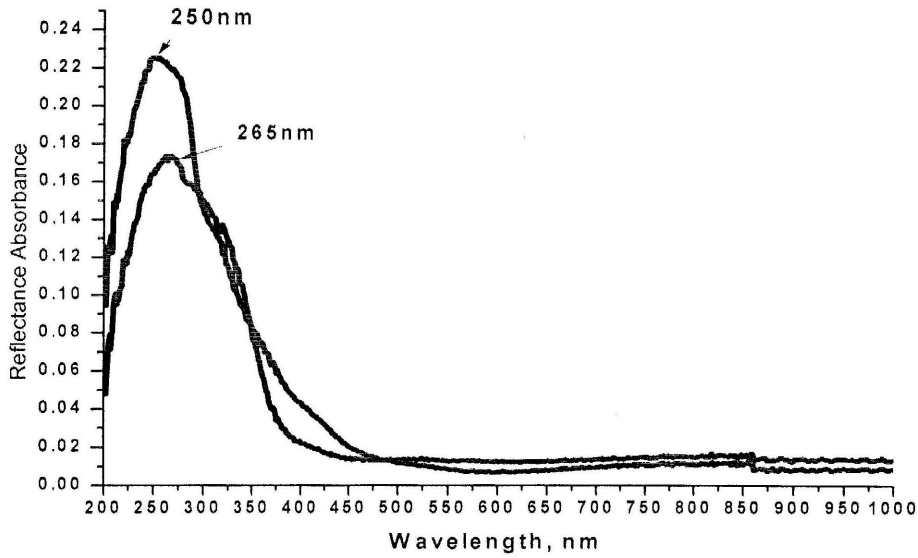

Figure 7. Solid state diffuse reflectance spectra of the metallopolymer PVPAu^{I}Cl(black) and the polymer PVP(red).

Time resolved measurements (Figure 8) is strong evidence for the presence of interchain and intrachain interaction and site-selective excitation of the metallopolymer. Initially at 0.00 delay, an emission peak was observed in both 1:1 and 1:10 metal to polymer ratios with λ_{max} at 470 nm. Upon increasing the delay time, this blue peak fade away and a new 560 nm yellow peak was seen after 70.0 μs delay for the ratio of 1:1 and 50.0 μs delay for the 1:10 metal to polymer molar ratio. The change accrued gradually with good correlation between the delay of the blue peak and the rise of the yellow peak, remarkably manifesting energy transfer between the multiple color sites in the metallopolymer.

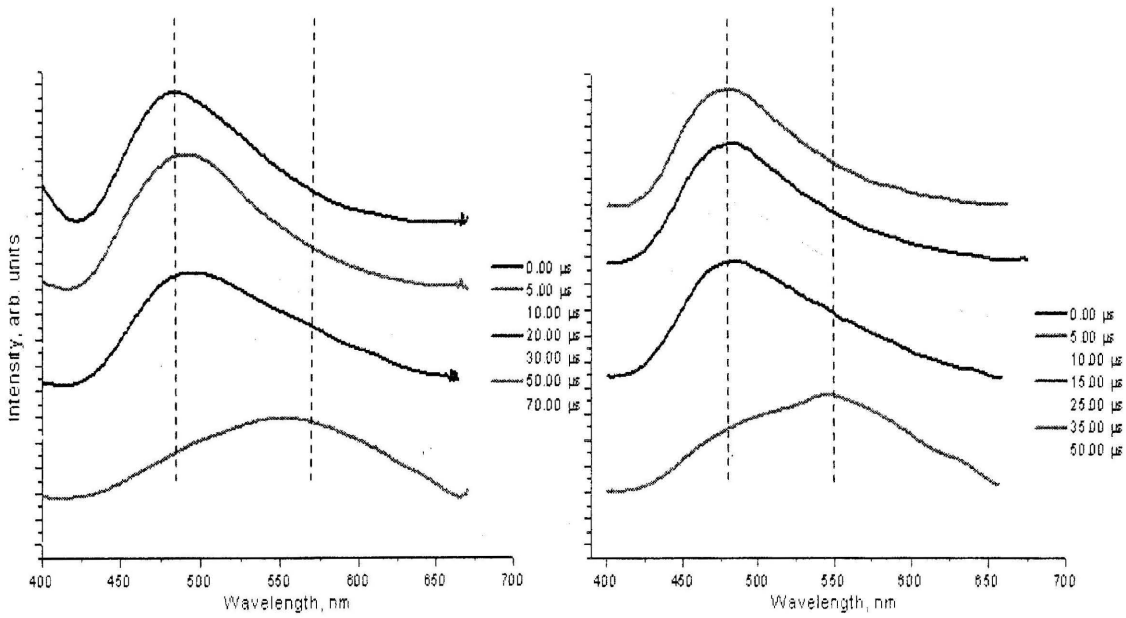

Figure 8. room temperature solid state time resolve PL of the metallopolymer 1:1 PVP-Au^{I}Cl (left) and 10:1 PVP-Au^{I}Cl (right).

Figure 9 shows ^{1}HNMR titration measurement is an interesting illustration of formation of the golden metallopolymer. We observed the drop of the ^{1}H signals of the free polymer as we increased the gold content, which can be an evidenced in the formation of the insoluble metallopolymer PVP-Au^{I}Cl.

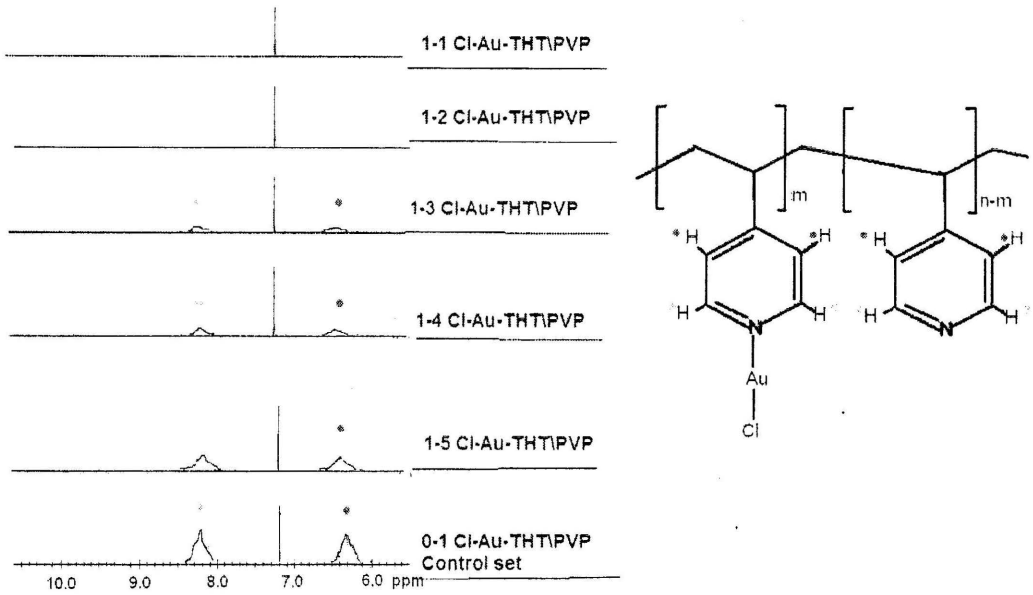

Figure 9. ^{1}HNMR spectra of the reaction of THT-Au^{I}Cl and PVP vs molar ratio in CDCl3. ^{1}H NMR shift Values are 6.40 and 8.3 ppm, respectively.

Altering the chloride-ligand with the chromophoric electron withdrawing moiety C_6X_5 (X= F, Cl) is expected to affect the energy levels and the transition probability (excitation coefficients and quantum yield) causing a change in both the excitation and emission spectra from these of the metallopolymer PVP-AuCl. That is, the blue emission changed to greenish emission at RT while a red shifted in the excitation maximum ware observed ($\lambda_{exc(C6F5AuPVP)}$=410nm). This shift is probably partially due to the decrease in the metal back bonding capability towards the σ-donating polymer. Temperature-dependent PL spectra and lifetimes of $C_6F_5Au^{I}PVP$ are shown in Figure 10. The bright PL of C_6F_5AuPVP in the solid state was fine tuned between four emission maxima (λ_{em}=510, 530, 550 and 570 nm) by varying λ_{exc} at all temperatures. This PL showed sensitivity of the luminescence energy, intensity and QY of the metallopolymer to the

temperature and site selective excitation. Upon raising the temperature to RT, the emission spactra was blue shifted to have maximum peak at 520 nm and become less sensitive to the excitation. Altering the fluoride ions in the phenyl group by the chloride ions led to the bright luminescent $C_6Cl_5Au^IPVP$. Figure 11 represents temperature-dependent PL and PL spectra and lifetimes of $C_6Cl_5Au^IPVP$ which can be fine tuned from the blue emission (λ_{em}=480nm) at 77K to yellow emission(λ_{em}=570nm) at RT. The unstructured emission with the microsecond lifetime obtained in both cases is consistent with metal-centered phosphorescence emission. However, the emission of $C_6Cl_5Au^IPVP$ blue shifted from the emission of $C_6F_5Au^IPVP$, while the 480 nm peak diminished at higher temperature and the 550 nm peaks increased in intensity upon varying excitation. The energy of emission bands of $C_6X_5Au^I$-PVP in general were red shifted from those of PVP-Au^ICl metallopolymer probably due to a change in Au—Au interaction and\or other steric and electronic effect of the different ligands. The larger size of the chlorinated phenyl ligand than the fluorinated phenyl causes steric interference which may lead to different Au--Au interactions. Our intuitive premise that stronger π-donor ligands will have lower absorption energy and X = Cl makes C_6X_5 a better π-donor then X=F since the assignment involved charge transfer from C_6X_5 to pyridine. Furthermore, Table 2 and 3 represent the photophysical measurements for $C_6F_5Au^I$-PVP and $C_6Cl_5Au^I$-PVP, respectively. In comparing Tables 2 and 3 data, $C_6F_5Au^I$-PVP shows higher QY value (63%) versus $C_6Cl_5Au^I$-PVP (28%) at 298 K and λ_{exc} = 410nm. The small increase in the lifetime and intensity of $C_6F_5Au^I$-PVP upon cooling to cryogenic temperature suggests

slight diminishing of nonradiative decay rate constant (2.58 X 10^5 s^{-1}) versus the radiative decay rate constant (4.46 X 10^5 s^{-1}) at RT.

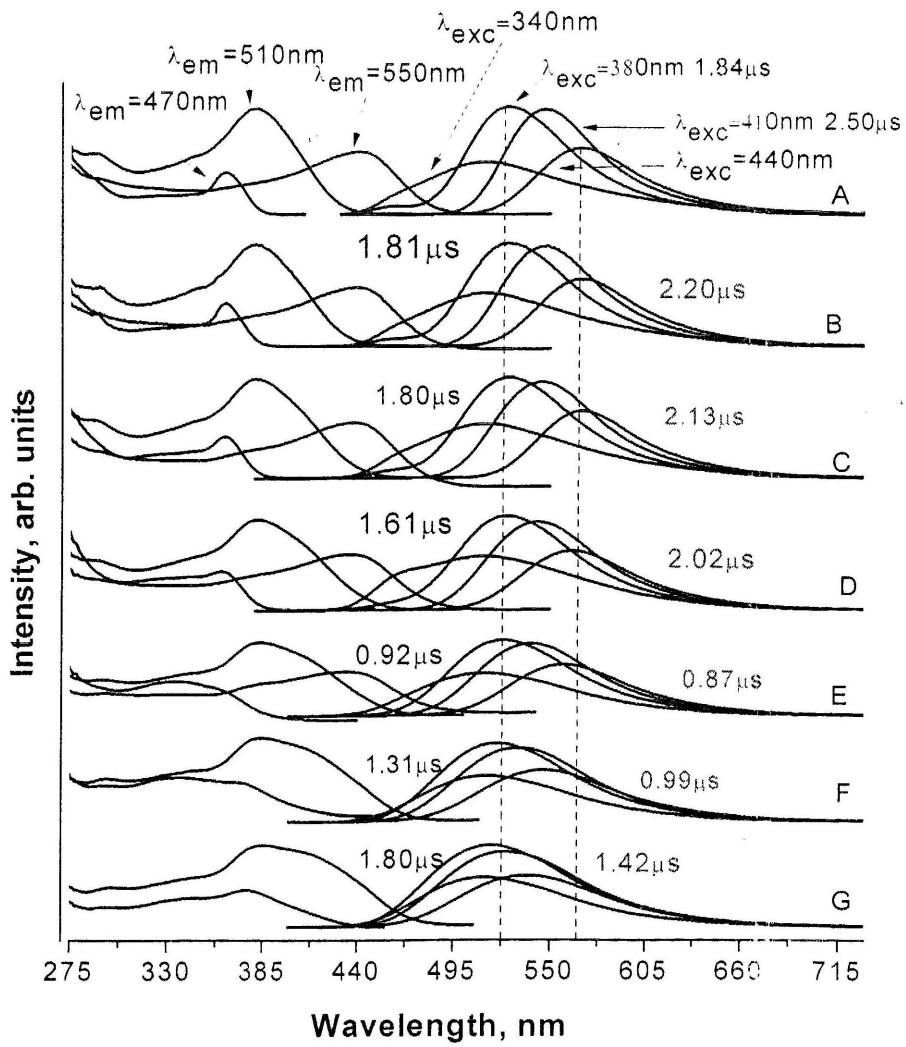

Figure 10. Solid state photoluminescence excitation (left) and emission (right) spectra at (A) 77K (B) 90K (C) 120K (D) 150K (E) 180 K (F) 235K and (G) 295K of PVP-Au^I-C_6F_5. The labeled spectra show the emission is red shifted upon varying excitation (340, 380, 410, and 440 nm respectively).

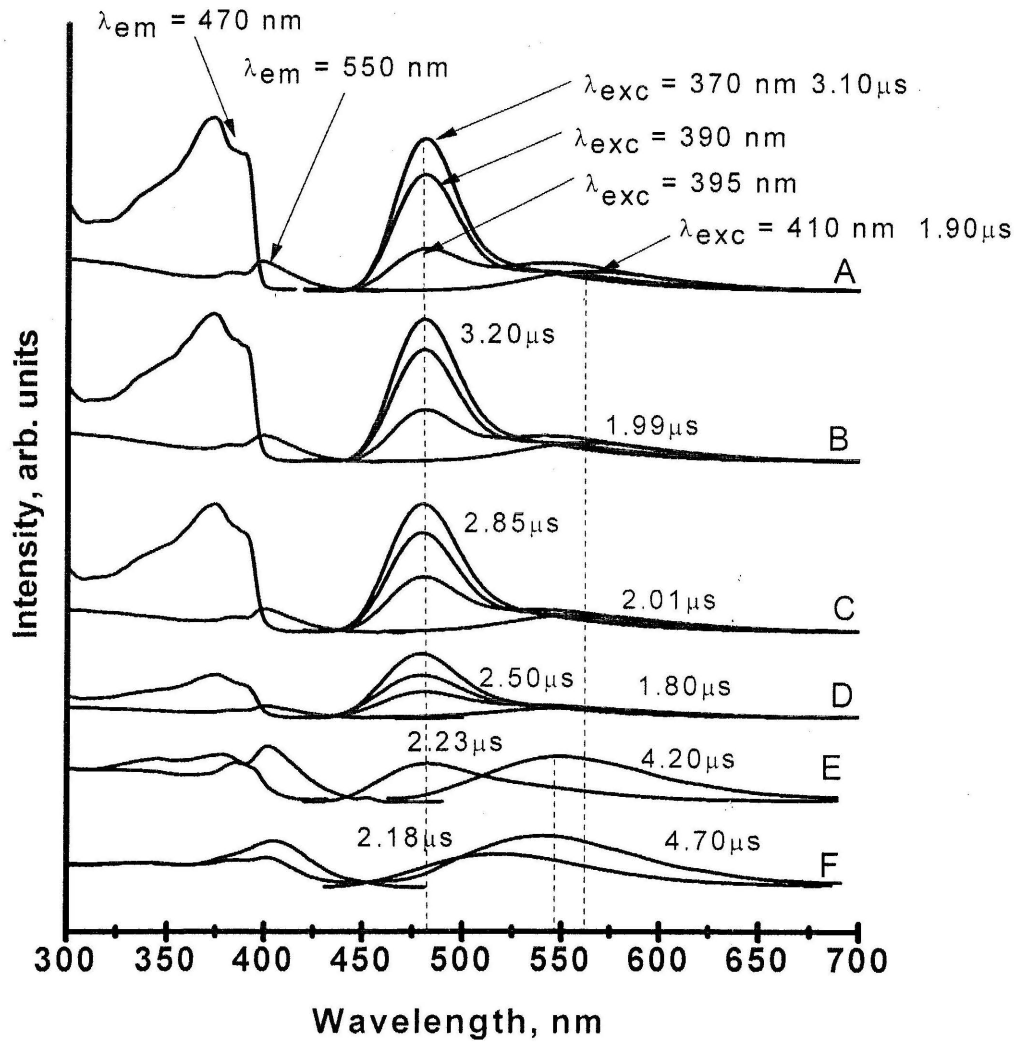

Figure 11. Photoluminescence excitation (left) and emission (right) spectra at (A) 77K (B) 90K (C) 120K (D) 150K (E) 210 K and (F) 295K for solid of PVP-Au^{I}-C_6Cl_5. The intensity of 480 nm peak is diminished at higher temperature while the peak at 550 nm grows upon varying excitation (370, 390, 395, and 410 nm respectively).

Table 2.

Temperature Dependent Photophysicals Parameters of Solid Samples of [Au^{I} (C_6F_5)PVP].

T(K)	Peak Area	Φ(%)	τ (μs)	$k_r(s^{-1})$	$k_{nr}(s^{-1})$
	[Au^{I} (C_6F_5)PVP] 410nm				
295	5.78E+08	63.4	1.42	4.46E+05	2.58E+05
235	5.29E+08	58	0.99	5.86E+05	4.24E+05
190	4.73E+08	51.9	0.87	5.96E+05	5.53E+05
150	5.56E+08	61	2.02	3.02E+05	1.93E+05
120	5.85E+08	64.2	2.13	3.01E+05	1.68E+05
90	5.79E+08	63.5	2.2	2.89E+05	1.66E+05
77	5.82E+08	63.8	2.5	2.55E+05	1.45E+05
	[Au^{I} (C_6F_5)PVP]	270nm			
295	6.18E+08	59.8	1.8	3.32E+05	2.23E+05
235	5.66E+08	54.8	1.31	4.18E+05	3.45E+05
190	5.18E+08	50.2	0.92	5.45E+05	5.42E+05
150	6.28E+08	60.8	1.61	3.78E+05	2.43E+05
120	6.54E+08	63.3	1.8	3.52E+05	2.04E+05

Table 3.

Temperature Dependent Photophysical Parameters of Solid Samples of [Au^{I} (C_6Cl_5)PVP].

T(K)	Peak Area	Φ(%)	τ (μs)	$k_r(s^{-1})$	$k_{nr}(s^{-1})$
	[Au^{I} (C_6Cl_5)PVP]	410nm			
295	1.51E+08	28.3	4.7	6.02E+04	1.53E+05
210	1.43E+08	24.7	7.2	5.89E+04	1.79E+05
150	1.72E+08	5.4	1.8	2.99E+04	5.26E+05
120	3.17E+08	9.3	2.01	4.63E+04	4.51E+05
90	3.32E+08	10	1.99	5.01E+04	4.52E+05
77	3.34E+08	10	1.9	5.26E+04	4.74E+05
	[Au^{I} (C_6Cl_5)PVP]	280nm			
295	1.51E+08	26.7	2.18	1.22E+05	3.36E+05
210	1.43E+08	25.4	2.23	1.14E+05	3.35E+05
150	1.72E+08	30.4	2.5	1.22E+05	2.78E+05
120	3.17E+08	56.2	2.85	1.97E+05	1.54E+05
90	3.32E+08	58.9	3.2	1.84E+05	1.29E+05
77	3.34E+08	59.2	3.1	1.91E+05	1.32E+05

Figure 12 represents the diffuse reflectance spectra of the metallopolymer $C_6F_5Au^{I}PVP$ in the solid state which exhibits several intense absorption bands between 240-350 nm and a weak band at 410 nm. The absorption band at 240 nm stems most likely from л-л* transition of the coordinated PVP polymer which shows a similar band between 250 -300 nm. The additional red shifted absorptions in $C_6F_5Au^{I}PVP$ vs. PVP or Cl-Au-PVP are caused by the π-conjugated chromophoric ligand, C_6F_5, and its mixing with Au(I) orbitals($d_л = d_{xz}, d_{yz}$). Following the literature reviews of small two coordinate linear gold(I) system (C_6F_5AuPy)[73], we assigned the band at 350 nm to charge transfer from the F_5C_6Au to PVP that is LMLCT.

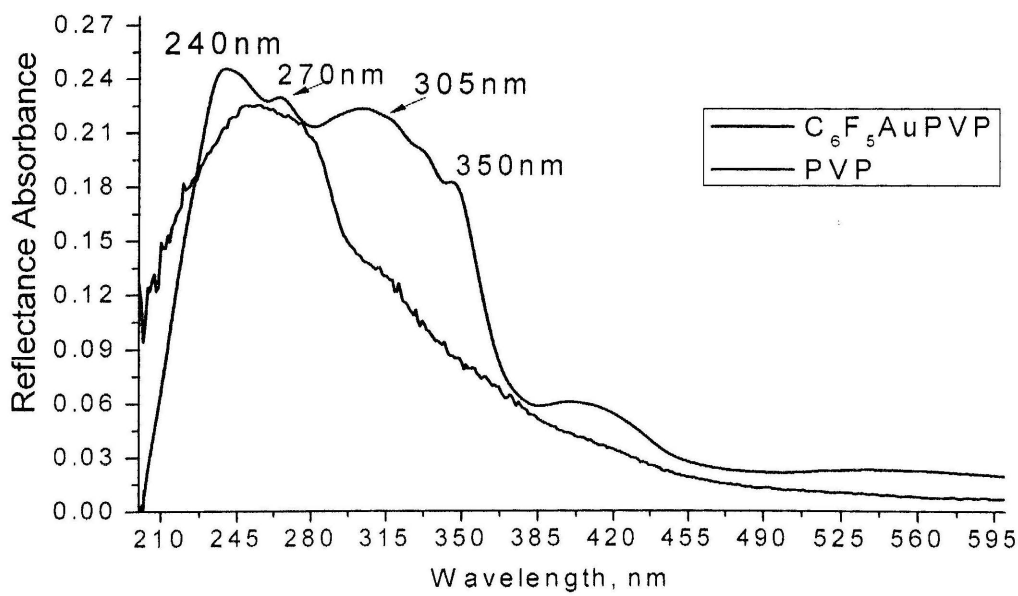

Figure 12. Solid state diffuse reflectance spectra of the metallopolymer $F_5C_6Au^{I}PVP$ (black) and the polymer PVP (red).

Shifting the electronic properties of the ligand from the electron poor $C_6X_5^-$ moiety to the electron rich ligand phenylacetylene led to a red shifted photoluminescent $C_6H_5CCAu^I$-PVP metallopolymer. In addition to the photoluminescence activity of the metallopolymer, the new starting material $C_6H_5CCAu^ITHT$ was also luminescent by itself. Figure 13 represents temperature dependent PL of the complex $C_6H_5CCAu^ITHT$ in which tunable emissions were obtained versus temperature with a lifetime emission of 6.31μs at cryogenic temperature and 4.21μs at room temperature. The bright PL of $C_6H_5CCAu^ITHT$ in the solid state was fine tuned between four emission maxima (λ_{em}=570, 585, 610 and 630nm) by varying λ_{exc} (Figure 13). The unstructured emissions with microsecond lifetimes reveal triplet state phosphorescent emission. On the other hand, coordination of $C_6H_5CCAu^ITHT$ to the PVP polymer resulted in a metallopolymer with interesting PL spectra. Figure 14 represents temperature-dependent PL spectra of the metallopolymer $C_6H_5CCAu^IPVP$. The PL of $C_6H_5CCAu^IPVP$ was fine tuned over a 50 nm range within the visible region, that is from green (λ_{em}= 520 nm) at 77 K to yellow luminescence (λ_{em}=630nm) at room temperature. This emission significantly red-shifted from the emission observed for metallopolymers PVP-AuCl, C_6F_5AuPVP, and C_6Cl_5AuPVP, corresponding with the new electron-releasing ligand C_6H_5CCAu. C_6H_5CC is a strong л-donor group causing red-shifted electronic transitions due to destabilized dл orbitals. The unstructured profile of the emission is consisting with Au-centered emission due to clustering of monomeric units.

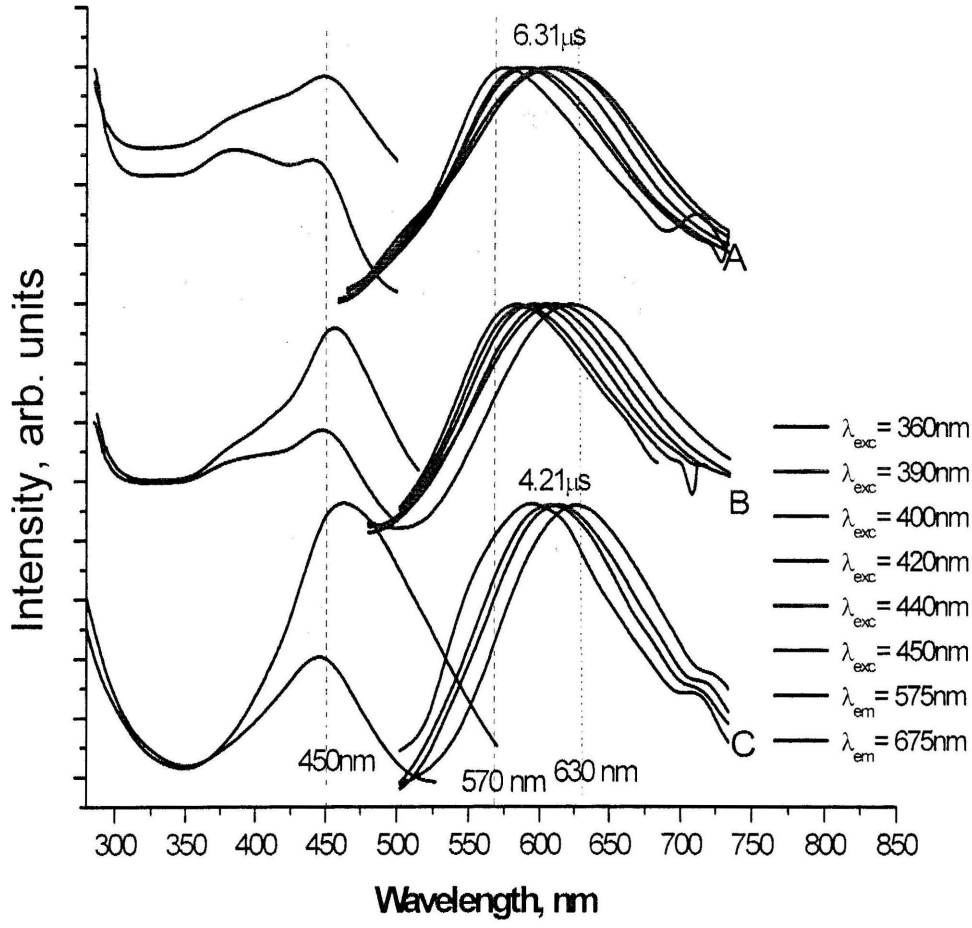

Figure 13. Photoluminescence excitation (left) and emission (right) spectra at (A) 77K (B) 180 K and (C) 295K of solid $C_6H_5CCAu^ITHT$. The spectra show the emission is red shifted upon varying excitation (360, 390, 400, 420, 440 and 450 nm, respectively).

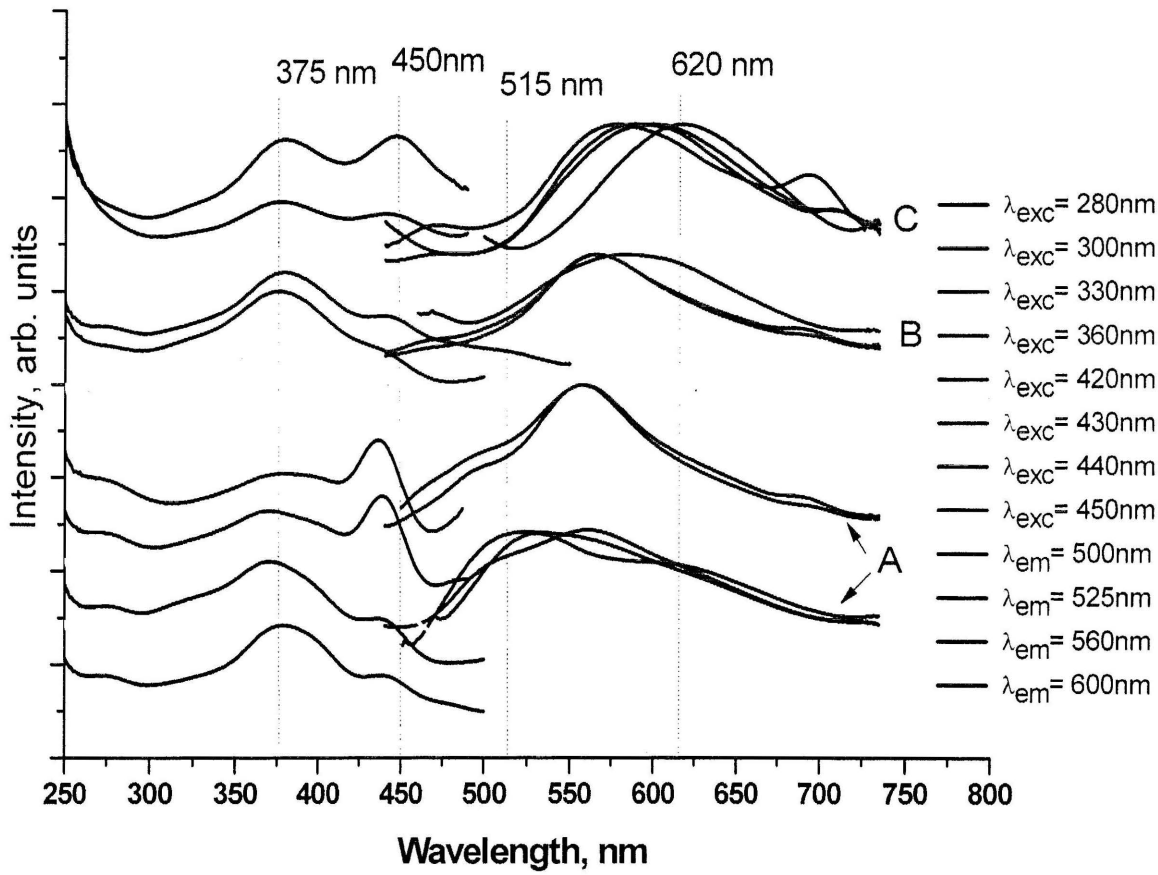

Figure 14. Photoluminescence excitation (left) and emission (right) spectra at (A) 77K (B) 180 K and (C) 295K of solid $C_6H_5CCAu^I$-PVP. The spectra show the emission is red shifted upon varying excitation (330, 360, 420, 430, 440 and 450 nm respectively).

Figure 15 represents the solid state diffuse reflectance spectra of the complex $C_6H_5CCAu^ITHT$ in which the peak at 290 nm corresponds to intraligand л-л* transition. The peak at 400 nm is likely due to ligand to metal charge transfer, that is from the л orbitals of the phenylacetylene to the gold atom's vacant 6p orbitals. On the other hand, the solid state diffuse reflectance spectra of the metallopolymer $C_6H_5CCAu^IPVP$ is represented in Figure 15. Following the literature reviews of small molecular regime

tBuCCAuCl[74,75], the HOMO has a CCAu mixed accetylide-metal character. Therefore, for $C_6H_5CCAu^{I}PVP$, we assign the electronic transition bands at 400 nm and 560 nm to LMLCT, from a C_6H_5CCAu HOMO to a PVP LUMO.

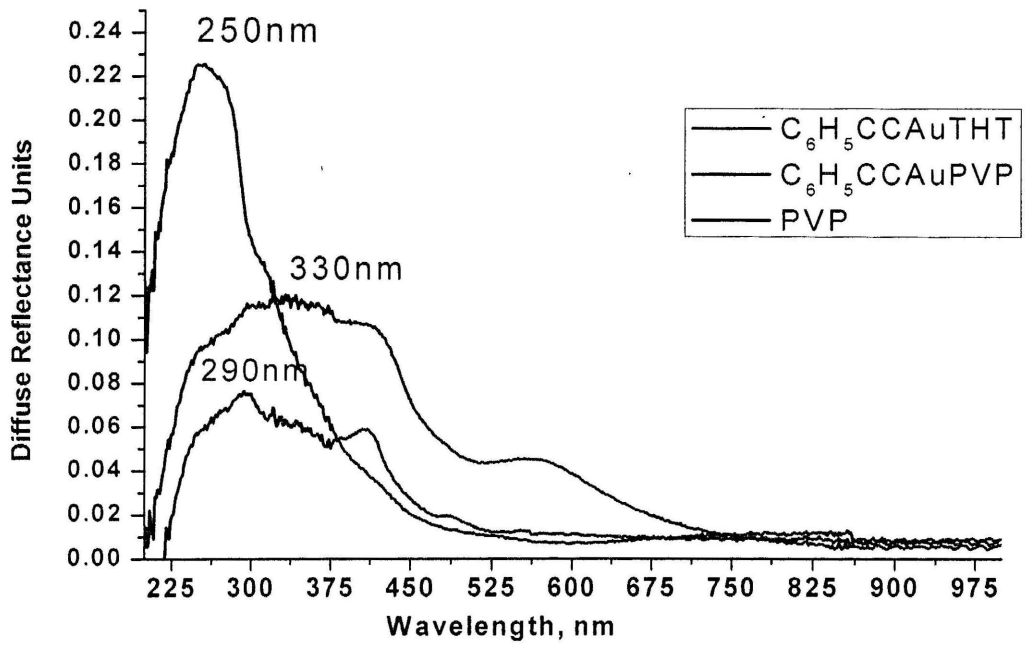

Figure 15. Solid state diffuse reflectance spectra of the complex $C_6H_5CCAu^{I}THT$(black) metallopolymer $C_6H_5CCAu^{I}PVP$(red) polymer PVP(blue).

In subsequent experimentation with the metallopolymer $C_6H_5CCAu^{I}PVP$, we changed the ligand C_6H_5CC to the electron poor (C_6F_5CC), which caused a blue shift in the absorption and emission bands of the metallopolymer $C_6F_5CCAu^{I}PVP$ when compared to the $C_6H_5CCAu^{I}PVP$. Figures 16 and 17 represent the PL and PLE spectra of both the complex and the metallopolymer $C_6F_5CCAu^{I}THT$ and $C_6F_5CCAu^{I}PVP$, respectively. The small complex $C_6F_5CCAu^{I}THT$ shows two emission peaks at λ_{max} =

530 nm and 575 nm in the green to yellow regions of the spectra. On other hand the metallopolymer $C_6F_5CCAu^IPVP$ exhibits a bright green PL in the solid state. Temperature-dependent PL spectra are shown in Figure 17. This PL emission is blue shifted (λ_{em}=540 nm and lifetime of 2.0 μs) from that of $C_6H_5CCAu^IPVP$ due to the electronic nature of the new fluorinated phenylacetylene ligand, wherein C_6F_5CC is a poorer л-donor than C_6H_5CC and thus has a lower HOMO. Microsecond lifetimes and unstructured emission spectra suggest triplet state phosphorescence from Au—Au bonded moieties (intrachain and\or interchain interaction).

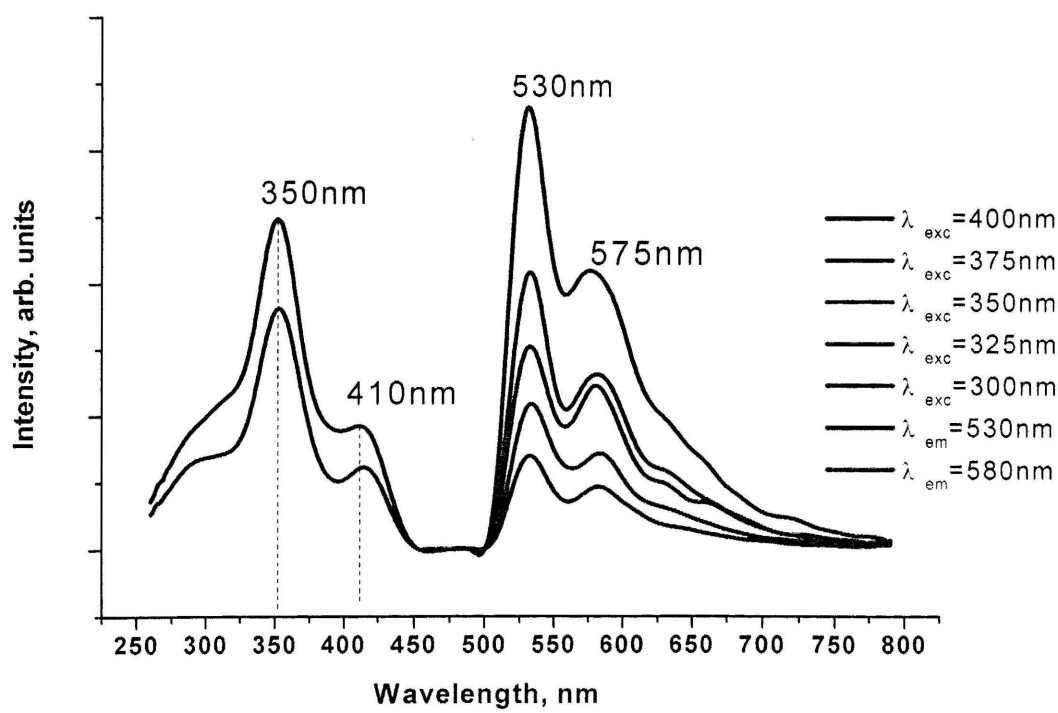

Figure 16. Photoluminescence excitation (left) and emission (right) spectra at 295K for solid $C_6F_5CCAu^ITHT$.

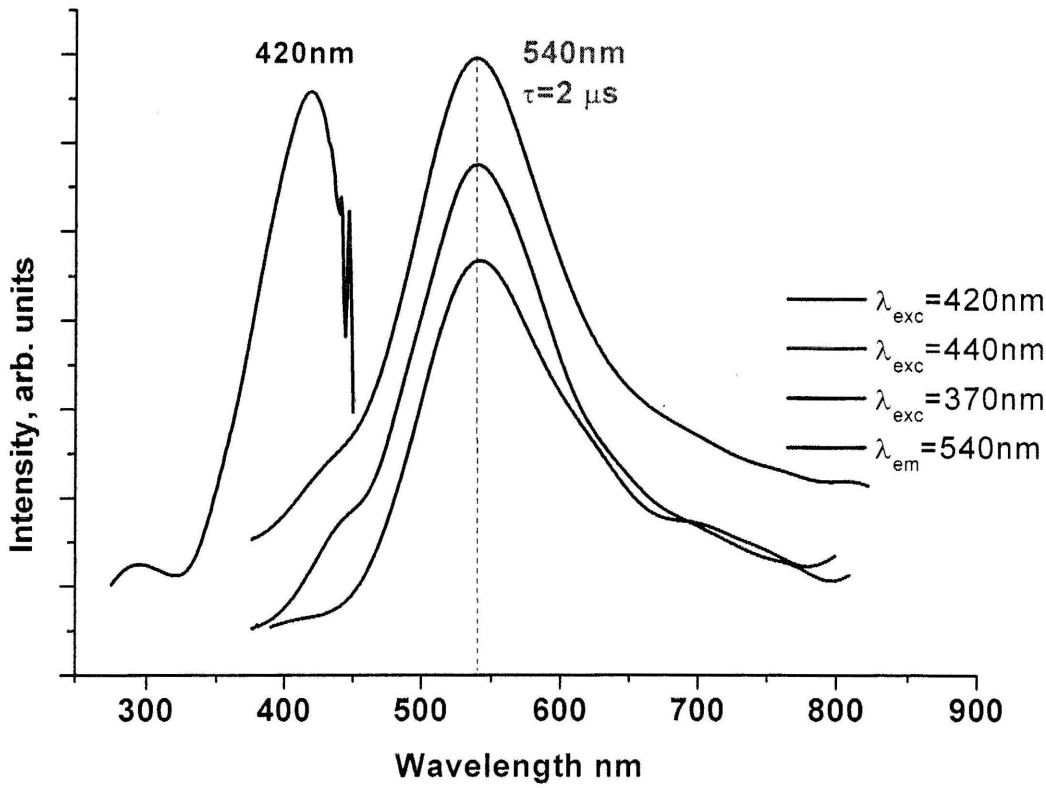

Figure 17. Photoluminescence excitation (left) and emission (right) spectra at 295K for solid $C_6F_5CCAu^IPVP$.

2.4 Conclusions

Direct coordination of small monovalent gold complexes to the polymer PVP led to a new class of luminescent metallopolymers with phosphorescent metal centered emissions at room temperature. Our focus was on studying the PL of the golden metallopolymers vs. ligand, temperature, and polymer:metal molar ratio and understanding how these factors influence the PL and other properties, as well as assessing the suitability of the new metallopolymers for potential PLED applications.

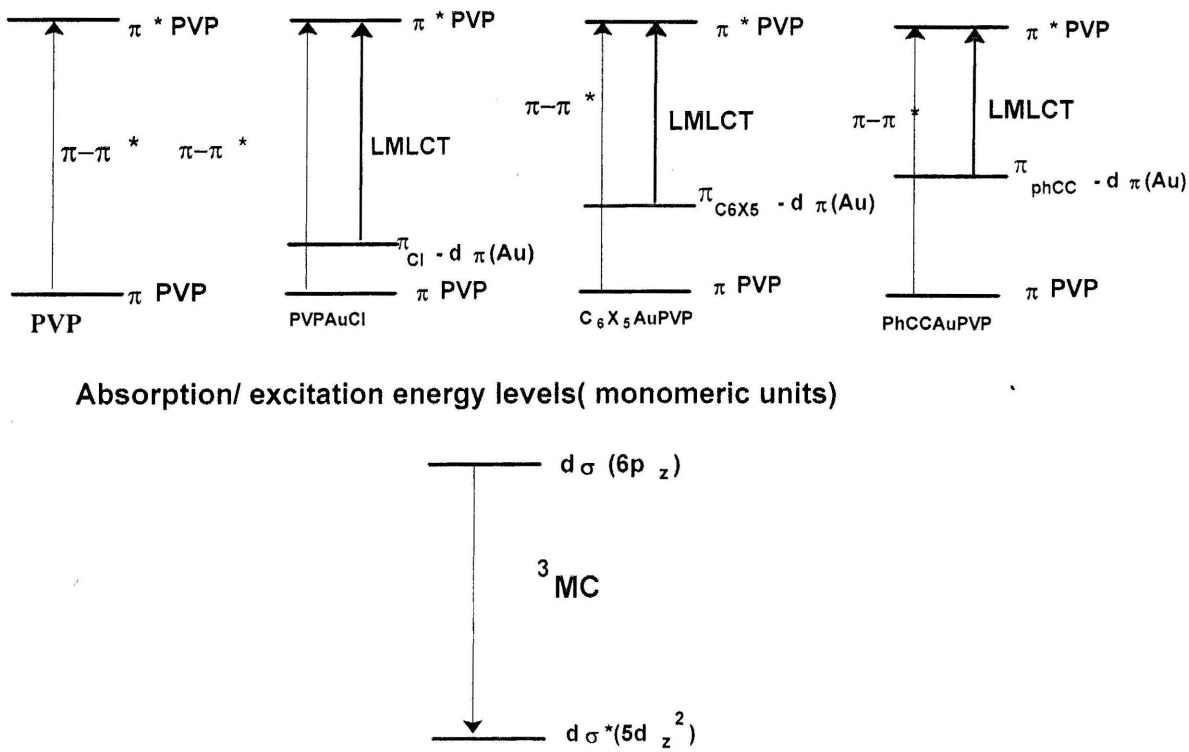

Figure 18. Illustrationof the HOMO LUMO absorption/excitation of the monomeric units (top) and emission energy levels of the excimeric Au – Au units (bottom).

Figure 18 illustrates the electronic transitions in monomeric units and emission energy levels in excimeric Au—Au units. For the monomeric units as we go from left to right the higher destabilization of the ligand orbitals occurs, causing a decrease in the HOMO LUMO energy levels between the metal and the polymer leading to the tunable excitation and absorption profiles discussed earlier. While the emission occurred from the deactivation of the excited triplet state of the excimeric units of gold. Thus from the bonding d_σ to antibonding d_σ^*. The metallopolymer PVPAuCl, with its bright blue luminescence (λ_{max}=480nm at 77K) and relatively low energy excitation (λ_{max}=375nm), could be considered as a good candidate for fabrication ofa high energy PLEDs device, but the extremely low solubility of this metallopolymer proved to be a hindrance in achieving this goal. In order to overcome this hurdle, we alternated the metal to polymer molar ratio to study the effects of metal content on the phosphorescence emission and the solubility of the metallopolymer. Although PVPAuCl showed a blue luminescence at low gold content (15.4%w/w based in 1:10 metal to polymer molar ratio), this result did not affect the solubility of PVPAuCl upon testing a variety of organic solvents with different polarity. Thus, even higher PVP:Au ratios than 10:1and\or other strategies should be investigated to overcome the solubility issue. On the other hand, replacing the Cl- ligand with the more electron poor ligand C_6X_6 led to a change in the luminescence and excitation maxima from those of the PVPAuCl. The emission and excitation peak maxima changed from 480 nm and 375 nm for the PVPAuCl, respectively, to 560 nm and 440 nm emission and excitation of C_6F_5AuPVP, while the C_6H_5CCAuPVP showed an orange and yellow photoluminescence at room and cryogenic temperatures. The change

in the luminescence maxima from those of the previous metallopolymers (PVPAuCl and C_6X_6AuPVP) by altering the ligand to see if that will achieve further tuning or alter the solubility led to the synthesis of the C_6F_5CCAuPVP metallopolymer. C_6F_5CCAuPVP showed green metal centered phosphorescence emission centered at 530 nm at room temperature. All of the metallopolymers showed bright photoluminescence at both room and cryogenic temperature with the emission covering most of the visible region (from 480 nm to 630 nm). The photoluminescence emission was assigned to metal centered triplet state phosphorescence emission.

We successfully un-silenced the non-phosphorescent polymer and starting material to obtain a phosphorescent metallopolymer at RT with high QY value for the same. For example, C6X5AuPVP, QY value of 63% at RT was achieved. the phosphorescent emissions was tuned across the visible region: blue(PVPAuCl), green (C6X5AuPVP), orange (phCCAuPVP). The combination of these emission colors is considered a recipe for white lighting application and the selective mixing of these metallopolymers leads to other intermediate colors, which is suitable for full-color displays applications (TV, Cell Phones, ect.). Furthermore, the aurophilic bonding in the polymers and the rare Au-N (soft-hard) bond are considerably important in the field of bonding chemistry.

Although the starting materials are highly soluble, the final metallopolymer products do not exhibit enough solubility in common organic solvents to allow spin coating of the material into thin films. Still suitable for sensor applications (temperature, vapor, pressure, etc.) that do not need high solubility. Strategies to circumvent this limitation by multiple chemical and physical means should be investigated. For example,

by introducing other long chain alkyl substituents into the polymer or anionic ligand, altering the d_{10} metal to Cu_I and/or Ag_I, doping in other non-coordinating polymer, and other means could be assessed.

CHAPTER III

THE SYNTHESIS CHARACTERIZATION AND SPECTROSCOPIC MEASUREMENTS OF MONOVALENT Ag(I) AND Cu(I) METALLOPOLYMERS

In this chapter we will discuss the synthesis, characterization and photoluminescence of silver(I) and copper(I) metallopolymers. The synthesis of silver(I) and copper(I) metallopolymer was attempted as a less expensive alternative to the analogous gold metallopolymers. The following sections cover the relevant topics. Section 3.1 goes over the chemicals and materials used in the synthesis of all the silver(I) and copper(I) metallopolymers . Section 3.2 presents in detail the synthetic methods used of silver and copper metallopolymer. Section 3.3 discusses the spectroscopic measurements obtained for the silver(I) and copper(I) metallopolymers. Finally section 3.4 summarizes the main conclusions and the prospective future direction about this project.

3.1 Chemicals and Materials

HPLC grade Acetonitrile, Tetrahydrofuran (THF), Dichloromethane (DCM), Methanol, Toluene and Benzene were purchased from Aldrich, and used after drying with conventional methods. Tetrafluoroboric acid (48% HBF_4), Silver(I) Oxide (Ag_2O), copper(I) oxide (Cu_2O) and poly-(4-vinylpyridene) (PVP) (AMW =60,000) were purchased from sigma Aldrich and used as is.

All reactions were carried out by Schlenk technique under inert atmospheric conditions unless indicated otherwise.

3.2 Syntheses

3.2.1 Synthesis of the Metallopolymer [[3,5-$(CF_3)_2$Pz]Ag]$_2$-{Poly(4-Vinyl)pyridine}$_2$.

$$Ag_2O + [3,5\text{-}(CF_3)_2Pz]H \longrightarrow [[3,5\text{-}(CF_3)_2Pz]Ag]_3$$

$$[[3,5\text{-}(CF_3)_2Pz]Ag]_3 + PVP \longrightarrow [[3,5\text{-}(CF_3)_2Pz]Ag\text{-}PVP]_2$$

With slight modification to literature methods[76-79]. Ag_2O (0.31 g, 1.35 mmol) and [3,5-$(CF_3)_2$Pz]H (0.5 g, 2.45 mmol) were mixed in about 20 ml benzene or toluene. The resulting mixture was protected from light using aluminum foil, and refluxed overnight. After cooling, the solution was filtered over a bed of Celite to remove some insoluble black material. The filtrate was collected and the solvent was removed under vacuum to obtain crude [80] as a colorless solid.

To a solution of {[3,5-$(CF_3)_2$Pz]Ag}$_3$ (0.200 g, 0.215 mmol) in 20.0ml dichloromethane, the stoichiometric ratio of PVP was added. The reaction mixture was

stirred for 1 hour and a white precipitate was formed and evaporated to dryness. Addition of 20 mL of dichloromethane and filtration led to a white solid (yield 85 %). FT-IR (KBr pellet): ν= 1615 cm^{-1} (C=N), ν= 3040 cm^{-1} (C=C-H aromatic) 2955 cm^{-1} (C-H Alkanes). Silver analysis (% wt): 22.00 % that correspond to 85.0% of PVP was occupied.

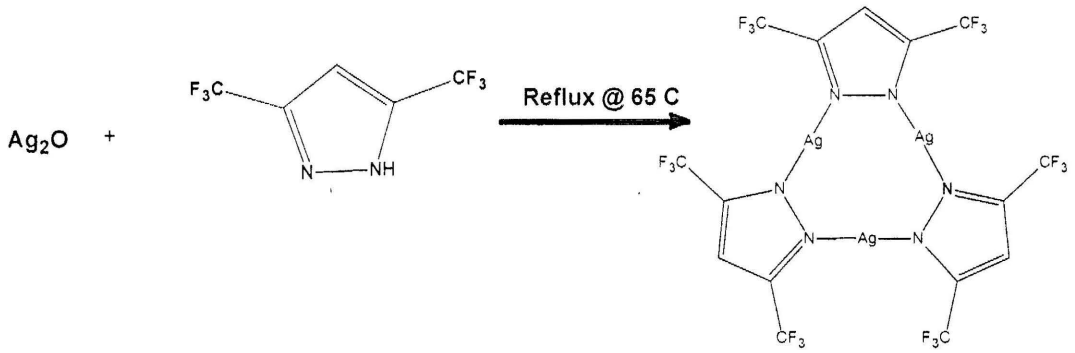

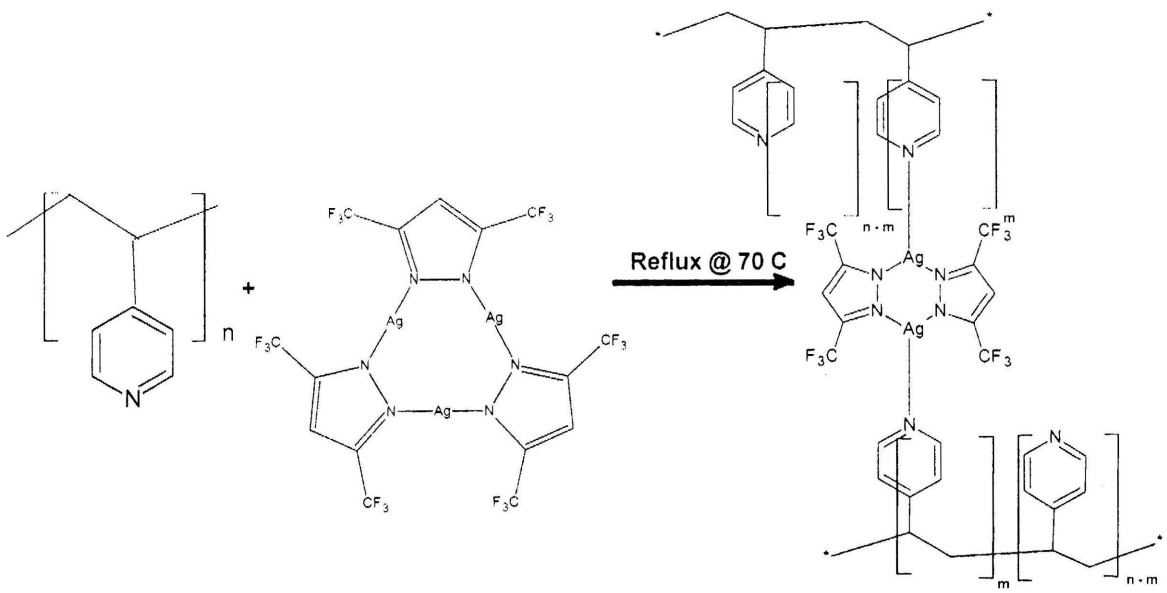

Figure 19. Illustration of synthetic route of ([3,5 $(CF_3)_2$Pz Ag^I- PVP]$_2$).

3.2.2 Syntheses of the Metallopolymer [Cu-(PVP)n][BF_4].

$Cu_2O + CH_3CN + HBF_4 \longrightarrow [Cu(CH_3CN)_4]BF_4$

$[Cu(CH_3CN)_4]BF_4 + PVP \longrightarrow [Cu\text{-}(PVP)n]BF_4$ n=1,2,3 or 4

With slight modification to literature methods[81-83],to a magnetically stirred solution of 4.0g (28 mmol) of Copper (I) oxide in 80 ml of Acetonitrile in a 150 ml schlenk flask is added 8 ml of 48% Tetrafluoroboric acid (HBF_4)(130 mmol) in 2 ml portions. The solution was stirred for 3 minutes and was then filtered hot through a medium porosity schlenk filter to remove small amounts of undissolved starting materials. To the pale-blue solution 100 ml of diethyl ether was added and cooled to freezing point for several hours, to form white-blue crystals of $[Cu(CH_3CN)_4][BF_4]$. The solid was collected by filtration, dissolved immediately in acetonitrile, recrystallized using diethyl ether , to obtain white crystals. Several recrystallizations may be needed to get the white crystals .The crystals were collected by filtration and washed with diethyl ether, dried under vacuum.

To a solution of $[Cu(CH_3CN)_4]$ BF_4(0.500 g, 1.590 mmol)(obtained in the reaction mentioned above) in 20 ml of toluene PVP (0.661 g, 6.360 mmol) was added. The reaction mixture was stirred for 2h and evaporated to dryness under vacuum. Addition of 20 mL of dichloromethane and filtration led to a yellow solid (yield 95 %). FT-IR (KBr pellet): ν= 1610 cm^{-1} (C=N), ν= 3040 cm^{-1} (C=C-H aromatic) 2950 cm^{-1} (C-H

Alkanes).Copper analysis (% wt): 8.88 %, that corresponds to 81.4% of occupied positions in the polymer.

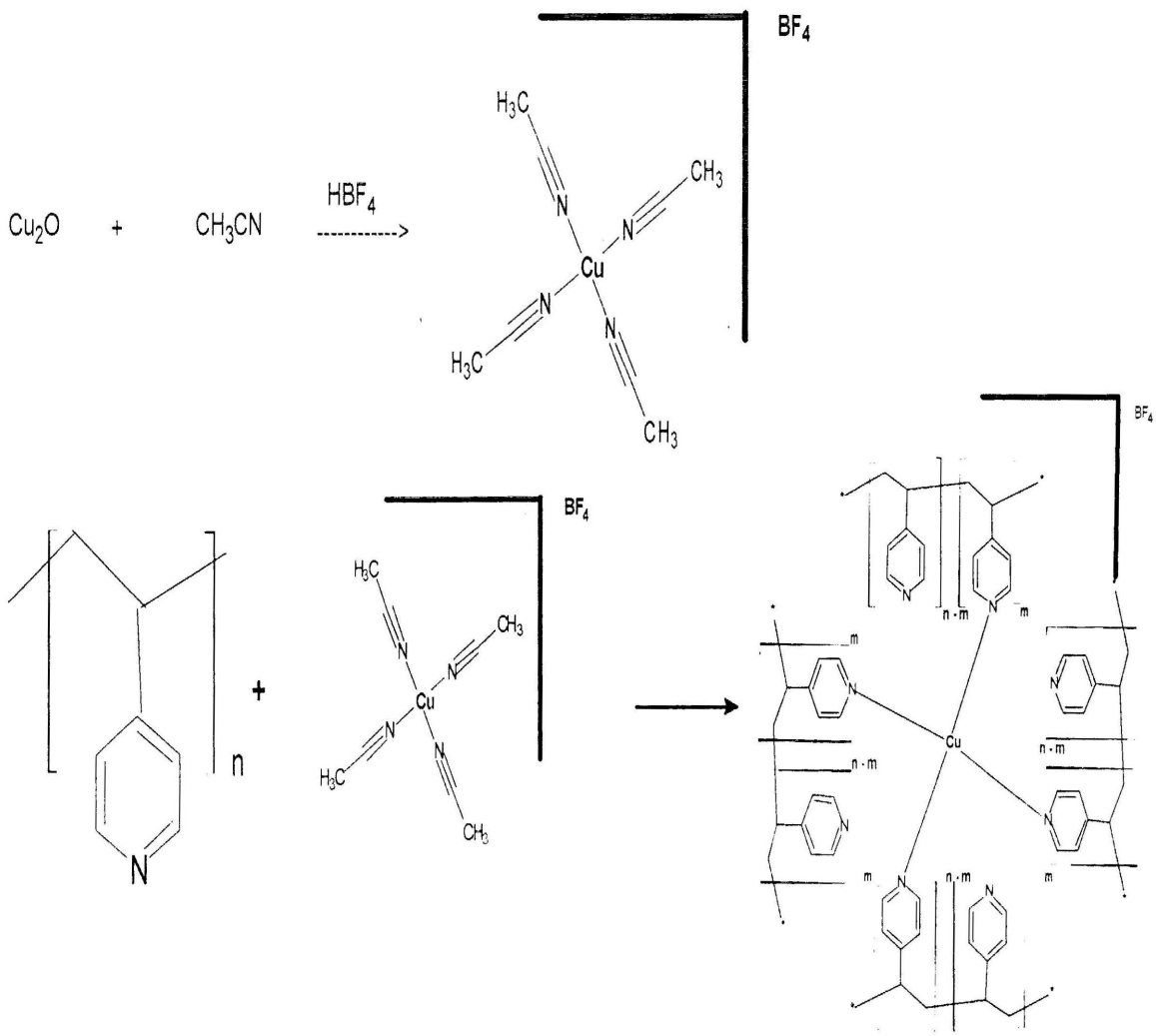

Figure 20. Illustration of the synthesis route of [Cu-(PVP)n]BF_4 metallopolymer

3.3 Result and Discussion

The reaction of the two coordinate small complex [3,5 $(CF_3)_2PzAg^I]_3$ with the PVP led to three coordinate silver(I) metallopolymer. Figure 18 is illustration of the suggested structure of silver(I) metallopolymer. This structure assumptions of the metallopolymer [3,5 $(CF_3)_2Pz\ Ag^I$- PVP]$_2$ were based on the literature reviews for three coordinate complexes of [3,5 $(CF_3)_2Pz\ Ag^I$ (2,4,6-collidine)}]$_2$ crystals[84].The new [3,5 $(CF_3)_2Pz\ Ag^I$-PVP]$_2$ metallopolymer exhibits bright blue photoluminescence (PL) in the solid state. Cryogenic and room temperature 1:3 and 1:8 molar ratio of metal to polymer PL and PL excitation (PLE) spectra and lifetimes are shown in Figure 21 and 22 respectively. These data reveal the sensitivity of the luminescence energies and intensities to both excitation wavelength and temperature. For Ag(I) metallopolymer, the emission can be tuned between two emission maxima (λ_{em}=460nm and 485nm) by varying λ_{exc} (λ_{exc}=300nm and 375nm) at the same temperature, that is both ratios of [3,5 $(CF_3)_2Pz\ Ag^I$- PVP]$_2$ metallopolymer shows two emission maxima at 460nm and 500nm upon varying the excitation energy and the temperature. At cryogenic temperature, the lifetime of this phosphorescence emission was calculated to be 2.4μs and 2.2μs for 1:3 and 1:8 molar ratios, respectively versus 1.6μs and 1.5μs lifetime at room temperature. The thermochromism luminescence and the microsecond scale unstructured emission indicates metal centered phosphorescence emission.

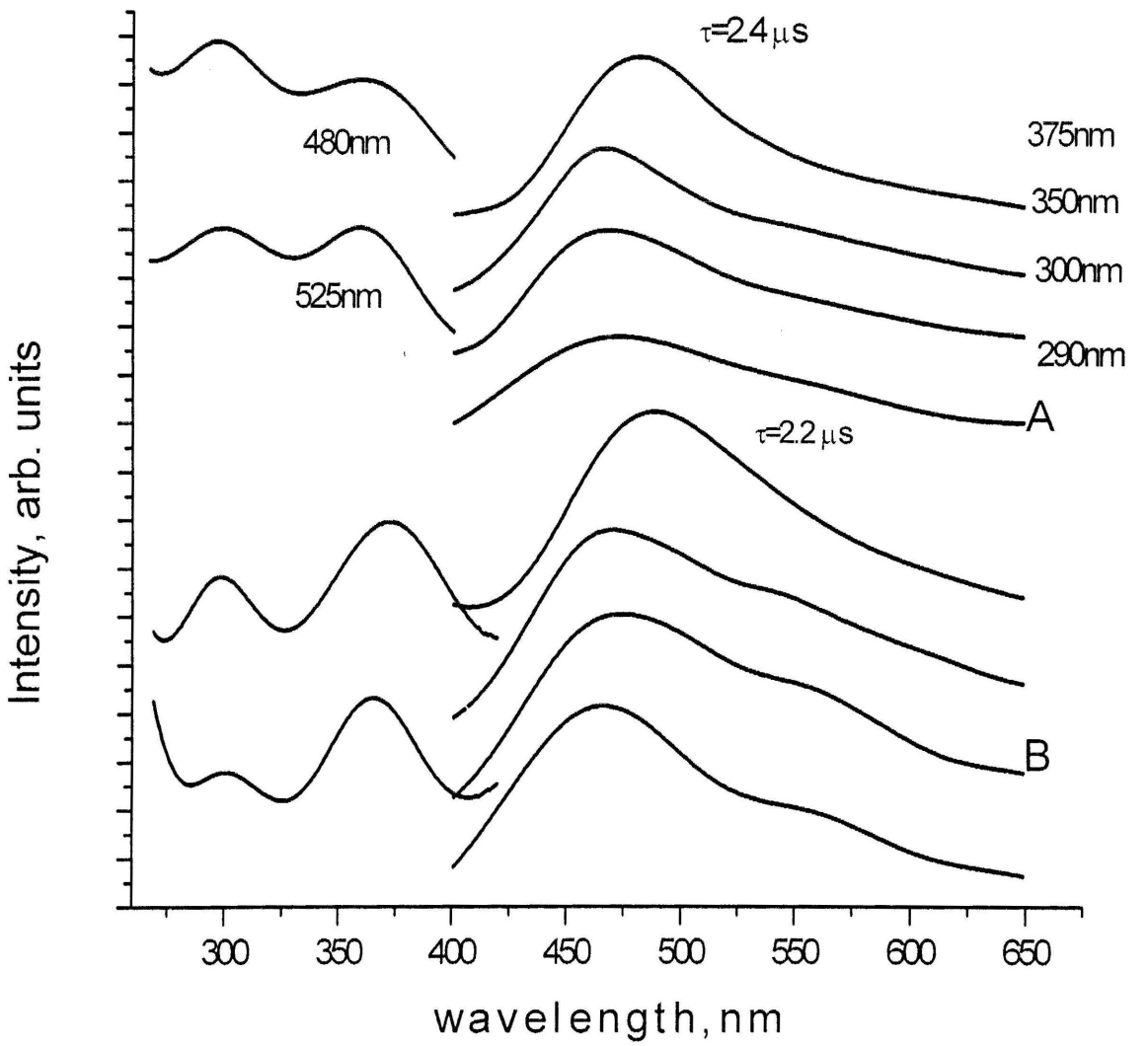

Figure 21. Photoluminescence excitation (left) and emission (right) spectra at (A) 77K ratio 1:3 (B) 77K ratio 1:8 of solid $[3,5\ (CF_3)_2Pz\ Ag^I\text{- }PVP]_2$ solid.

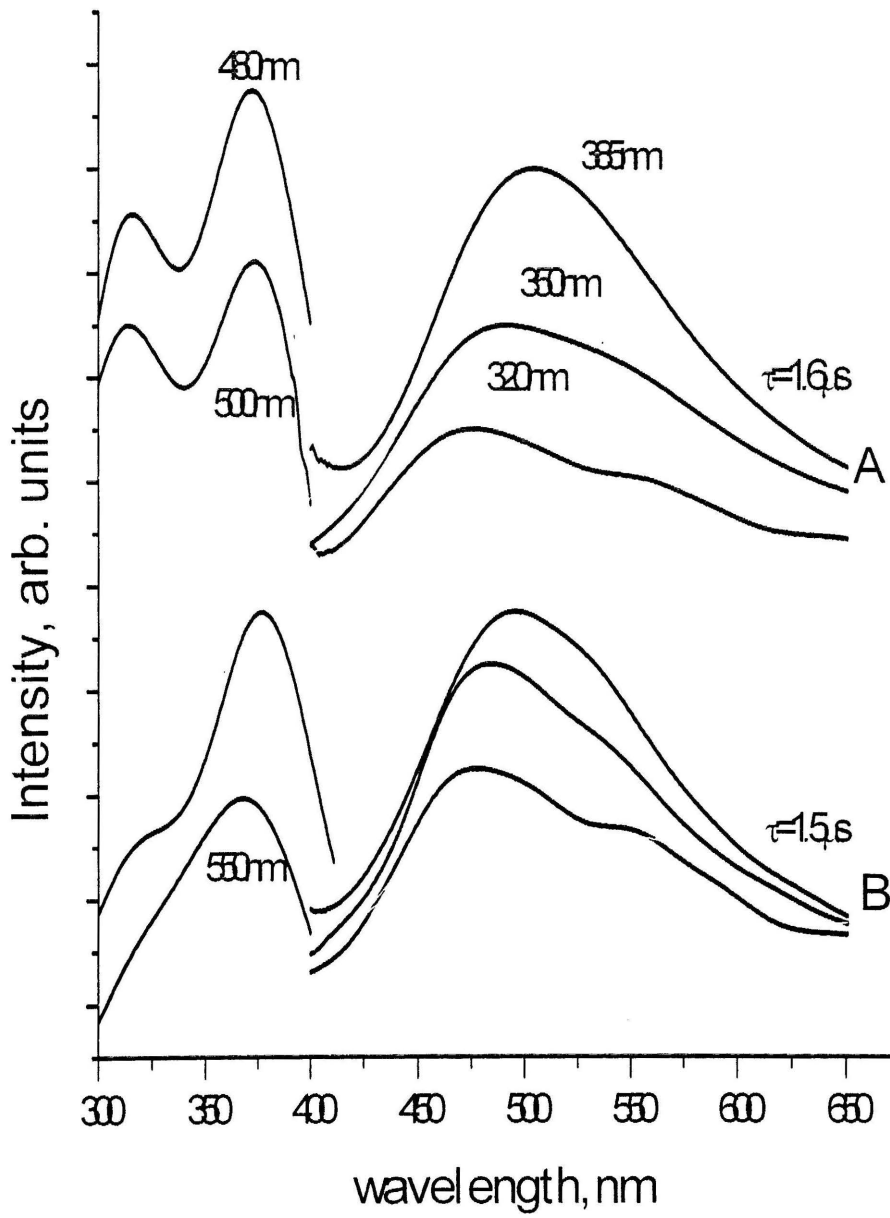

Figure 22. Photoluminescence excitation (left) and emission (right) spectra at (A) 298K ratio 1:3 (B) 298K ratio 1:8 of solid $[3,5\ (CF_3)_2Pz\ Ag^{I}\text{- }PVP]_2$ solid.

Solid state diffuse reflectance spectra (figure 23) show two peaks at 250 nm and 350nm. A literature report[84] for three coordinate complexes of silver(I) assigned the electronic transition in the small molecular regime [3,5 $(CF_3)_2$Pz Ag^I (2,4,6-collidine)$\}]_2$ to ligand to metal ($Pz\text{-}Ag^I$) charge transfer(LMCT)[84]. However, we prefer the same assignment for the Au(I) metallopolymers to assign the peak at 350nm as ligand metal ($Pz\text{-}Ag^I$) to ligand (PVP) charge transfer (LMLCT). Subsequently, we observed that changing the metal:polymer ratio has no significant effect.

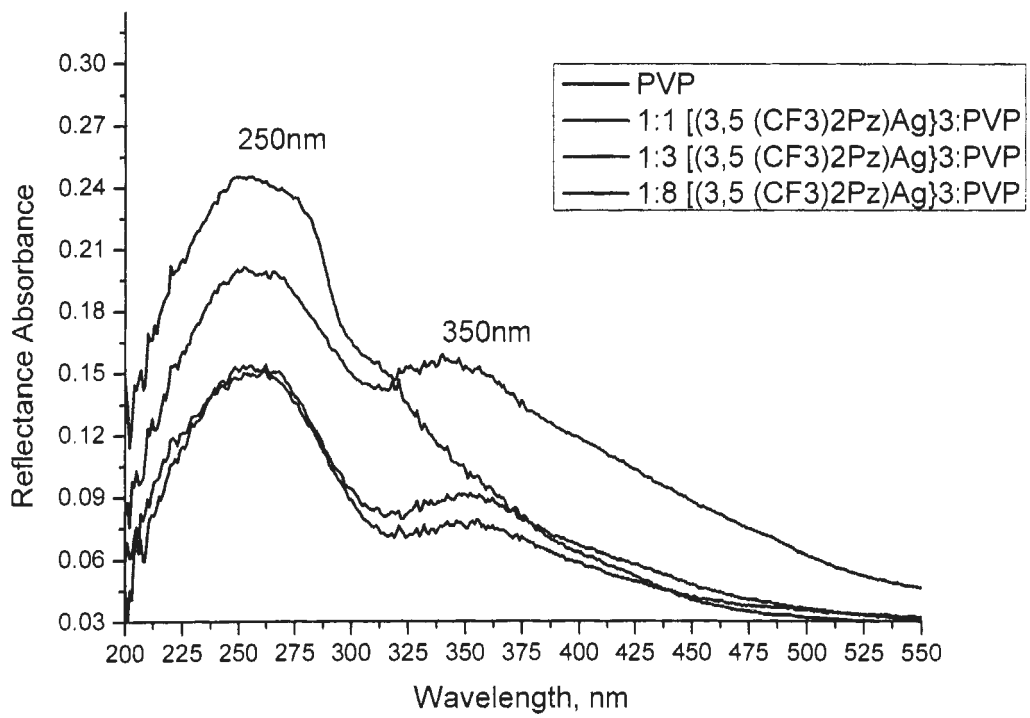

Figure 23. Solid state diffuse reflectance spectra of the metallopolymer [3,5 $(CF_3)_2$Pz Ag^I- PVP$]_2$.

In other route in the research we were able to synthesis four coordinate Cu(I) metallopolymer. The metallopolymer $[Cu^{I}\text{-}(PVP)_n].BF_4$ on the other hand exhibits a yellow (λ_{em}= 520-550nm) photoluminescence in the solid state. Cryogenic and room temperature PL for such metallopolymers with Cu:PVP molar ratio of 1:4 and 1:12 spectra and lifetimes are shown in Figures 24 and 25, respectively. Both set of spectra show excitation peak maxima at 405nm, emission peak maxima at 560nm and 575nm, and lifetime of 14.0μs for both molar ratios. These spectra reveal no sensitivity of the luminescence energies and intensities to the excitation wavelength. This metallopolymer was luminescent at cryogenic temperature only and no luminescence was observed at room temperature. While changing the molar ratio has an insignificant effect on the emission and excitation maxima of $[Cu^{I}\text{-}(PVP)n].BF_4$ metallopolymer (see Figures 24 and 25). The microseconds scale lifetime and unstructured emission indicates triplet state metal centered phosphorescence emission.

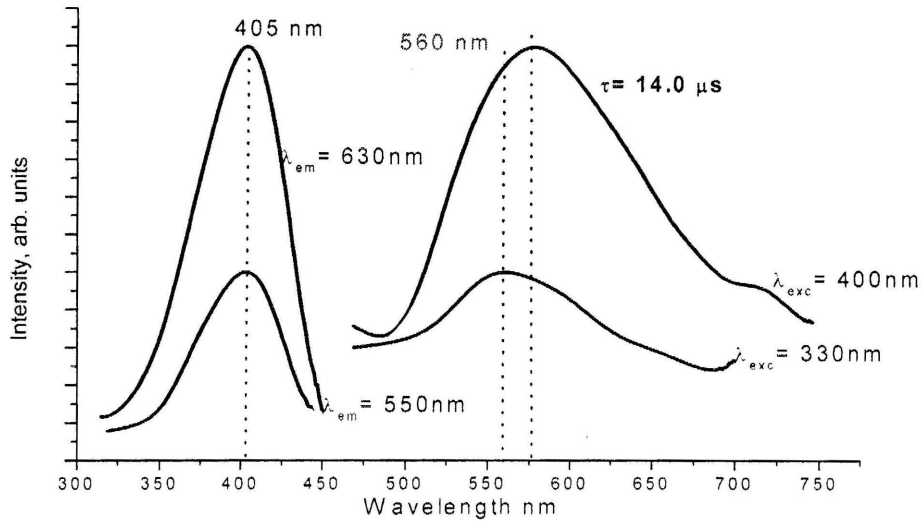

Figure 24. Photoluminescence excitation (left) and emission (right) spectra at 77K of solid $[Cu^{I}$ -(PVP)n].BF_4 in metal to polymer ratio of 1:4.

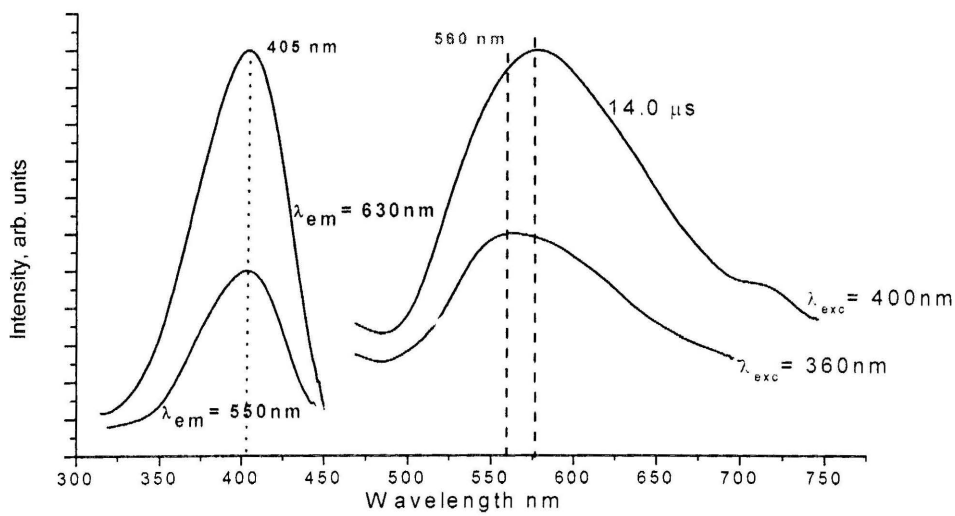

Figure 25. Photoluminescence excitation (left) and emission (right) spectra at 77K of solid $[Cu^{I}$ -(PVP)n].BF_4 in metal to polymer ratio of 1:12.

Figure 26 shows the diffuse reflectance spectra of the metallopolymer [Cu^{I} – (PVP)n].BF_4 measured in the solid state. The spectrum exhibits two bands at 255 nm and 330nm, and a shoulder extended until 500nm. The high energy band (250nm) raises intraligand transition of the PVP polymer. The shoulder centered at 450nm become less intense upon changing the ratio of the metal to the polymer to 1:12 respectively, suggesting metal to ligand charge transfer MLCT, this is because there is no л-donor anionic ligands like Cl^-, $C_6F_5^-$, $PhCC^-$. F_5PhCC^-, or Pz^- like those used in the other classes of metallopolymers studied in this thesis, which had LMLCT assignment and brighter PL bands.

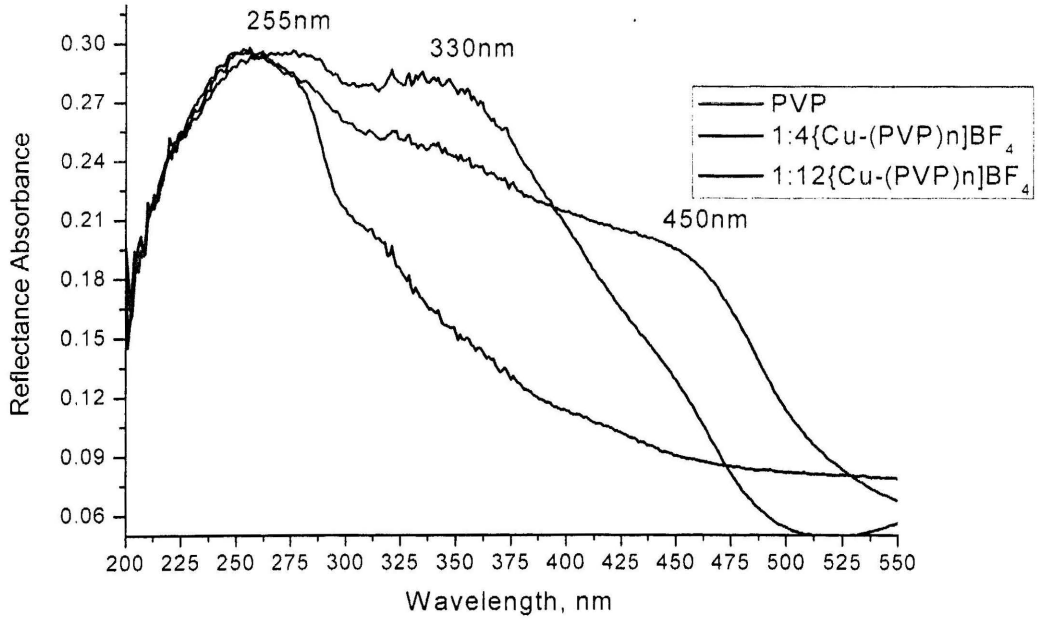

Figure 26. Solid state diffuse reflectance spectra of the metallopolymer [Cu^{I} – (PVP)n].BF_4.

3.4 Conclusions

To conclude, the results presented herein discuss the syntheses and photophysical properties of a novel class of phosphorescent copper and silver based metallopolymers. These phosphorescent metallopolymers can provide a cheaper and affordable replacement for the gold metallopolymers discussed in chapter two.

The spectra of the metallopolymer [3,5 $(CF_3)_2$Pz Ag^I- PVP]$_2$ shows two emission maxima at 460nm and 500nm with average lifetime of 2.3μs and 1.6 μs at 77K and 298K, respectively. This lies in the blue-green region of the spectrum. The excitation spectra also showed two excitation maxima at 300nm and 370nm. The microsecond scale unstructured emission indicates metal centered phosphorescence emission. On other hand the metallopolymer [Cu-(PVP)n]BF_4, showed yellow phosphorescent emission (λ_{em}= 550 nm) at 77K temperature with a lifetime of 14.0μs at low energy excitation band (λ_{exc}= 405nm). The low energy excitation suggests a smaller gap between the HOMO and LUMO levels. On other hand alternate metal to polymer molar ratio in both silver and copper metallopolymers led to no change in the excitation nor the emission spectrum.

We successfully un-silenced non-phosphorescent polymer to obtain bright phosphorescent metallopolymers at RT. The phosphorescent emissions were tuned across the visible region: blue([3,5(CF3)2PzAgPVP]2), yellow ([Cu-(PVP)n]BF4). Furthermore, the argentophilic and cuprophilic bonding in the polymers and the rare soft hard Ag-N and Cu-N bond are considered rare in field of bonding chemistry.

Efforts will be pursued to evaluate the performance of this class of Cu(I) and Ag(I) metallopolymers thereof as an alternative to the Au(I) metallopolymers PLED phosphors.

Although we were unable to overcome the solubility problem this metallopolymers specially Cu(I) open a potential use in presser and temperature sensors

REFERENCES

(1) Curie, D. *Luminescence in crystals*; Methuen;Wiley: London,New York,, 1963.

(2) Bowen, E. J. *Luminescence in chemistry*; Van Nostrand: London, Princeton, N.J.,, 1968.

(3) Lumb, M. D. *Luminescence spectroscopy*; Academic Press: London ; New York, 1978.

(4) Farnau, E. F. *Luminescence* [Ithaca, N.Y.], 1913.

(5) Faraday society, L. *Luminescence; a general discussion*; Published for the Faraday society by Gurney and Jackson: London [etc.], 1939.

(6) De Ment, J. *Fluorochemistry: a comprehensive study embracing the theory and applications of luminescence and radiation in physico-chemical science*; Chemical publishing company, inc.: Brooklyn, N.Y.,, 1945.

(7) Vij, D. R. *Luminescence of solids*; Plenum Press: New York, 1998.

(8) Skoog, D. A.; Holler, F. J.; Crouch, S. R. *Principles of instrumental analysis*; 6th ed.; Thomson Brooks/Cole: Belmont, CA, 2007.

(9) Ronda, C. R. *Luminescence : from theory to applications*; Wiley-VCH: Weinheim, 2008.

(10) John C. de Mello, H. F. W., Richard H. Friend, *Advanced Materials* **1997**, *9*, 230-232.

(11) Cioslowski, J. *Quantum-mechanical prediction of thermochemical data*; Kluwer Academic Publishers: Dordrecht ; Boston, 2001.

(12) Fery-Forgues, S.; Lavabre, D. *J. ChemEd* **1999**, *76*, 1260-64.

(13) Bagnoli, F.; DellaAmico, D. B.; Calderazzo, F.; Englert, U.; Marchetti, F.; Herberich, G. E.; Pasqualetti, N.; Ramello, S. *J. Chem. Soc., Dalton Trans.* **1996**, 4317.

(14) Reynolds, G. A.; Drexhage, K. H. *Optics Communications* **1975**, *13*, 222-225.

(15) Xu, Y.; Liang, B.; Peng, J.; Niu, Q.; Huang, W.; Wang, J. *Organic Electronics* **2007**, *8*, 535-539.

(16) Elbjeirami, O.; Yockel, S.; Campana, C. F.; Wilson, A. K.; Omary, M. A. *Organometallics* **2007**, *26*, 2550-2560.

(17) van Dijken, A.; Bastiaansen, J. J. A. M.; Kiggen, N. M. M.; Langeveld, B. M. W.; Rothe, C.; Monkman, A.; Bach, I.; Stossel, P.; Brunner, K. *Journal of the American Chemical Society* **2004**, *126*, 7718-7727.

(18) Hanna, S. D.; Khan, S. I.; Zink, J. I. *Inorganic Chemistry* **1996**, *35*, 5813-5819.

(19) Narayanaswamy, R.; Young, M. A.; Parkhurst, E.; Ouellette, M.; Kerr, M. E.; Ho, D. M.; Elder, R. C.; Bruce, A. E.; Bruce, M. R. M. *Inorganic Chemistry* **1993**, *32*, 2506-2517.

(20) Rawashdeh-Omary, M. A.; Omary, M. A.; Patterson, H. H. *Journal of the American Chemical Society* **2000**, *122*, 10371-10380.

(21) Rawashdeh-Omary, M. A.; Omary, M. A.; Fackler, J. P. *Inorganica Chimica Acta* **2002**, *334*, 376-384.

(22) Omary, M. A.; Rawashdeh-Omary, M. A.; Gonser, M. W. A.; Elbjeirami, O.; Grimes, T.; Cundari, T. R.; Diyabalanage, H. V. K.; Gamage, C. S. P.; Dias, H. V. R. *Inorganic Chemistry* **2005**, *44*, 8200-8210.

(23) Rawashdeh-Omary, M. A.; Omary, M. A.; Fackler, J. P.; Galassi, R.; Pietroni, B. R.; Burini, A. *Journal of the American Chemical Society* **2001**, *123*, 9689-9691.

(24) Rawashdeh-Omary, M. A.; Omary, M. A.; Patterson, H. H.; Fackler, J. P. *Journal of the American Chemical Society* **2001**, *123*, 11237-11247.

(25) Mohamed, A. A.; Rawashdeh-Omary, M. A.; Omary, M. A.; Fackler, J. P.; Jr. *Dalton Transactions* **2005**, 2597-2602.

(26) Mohamed, A. A.; Galassi, R.; Papa, F.; Burini, A.; Fackler, J. P. *Inorganic Chemistry* **2006**, *45*, 7770-7776.

(27) Bondi, A. *J. Phys. Chem.* **1964**, *68*, 441.

(28) Fackler, J. P.; Assefa, Z.; Forward, J. M.; Staples, R. J. *Met Based Drugs* **1994**, *1*, 459-66.

(29) Alfredo, B.; Rossana, G.; Bianca, R. P.; Alfredo, B.; Fackler, J. P. J.; Rossana, G.; Richard J. Staples *Chem. Commun.* **1998**, 95-6.

(30) Roundhill, D. M.; Fackler, J. P. *Optoelectronic properties of inorganic compounds*; Plenum Press: New York, 1999.

(31) Omary, M. A.; Rawashdeh-Omary, M. A.; Gonser, M. W.; Elbjeirami, O.; Grimes, T.; Cundari, T. R.; Diyabalanage, H. V.; Gamage, C. S.; Dias, H. V. *Inorg Chem* **2005**, *44*, 8200-10.

(32) Omary, M. A.; Rawashdeh-Omary, M. A.; Diyabalanage, H. V.; Dias, H. V. *Inorg Chem* **2003**, *42*, 8612-4.

(33) Dias, H. V. R.; Diyabalanage, H. V. K.; Eldabaja, M. G.; Elbjeirami, O.; Rawashdeh-Omary, M. A.; Omary, M. A. *Journal of the American Chemical Society* **2005**, *127*, 7489-7501.

(34) Dias, H. V. R.; Diyabalanage, H. V. K.; Rawashdeh-Omary, M. A.; Franzman, M. A.; Omary, M. A. *Journal of the American Chemical Society* **2003**, *125*, 12072-12073.

(35) Grimes, T.; Omary, M. A.; Dias, H. V.; Cundari, T. R. *J Phys Chem A* **2006**, *110*, 5823-30.

(36) Vorontsov, I. I.; Kovalevsky, A.; Yu; Graber, T.; Novozhilova, I. V.; Omary, M. A.; Coppens, P. *Phys. Rev. Lett.* **2005**, *94*, 193003.

(37) White-Morris, R. L.; Olmstead, M. M.; Attar, S.; Balch, A. L. *Inorganic Chemistry* **2005**, *44*, 5021-5029.

(38) Jess, C. V.; Marilyn, M. O.; Ella, Y. F.; Alan, L. B. *Angewandte Chemie* **1997**, *109*, 1227-1229.

(39) H. V. Rasika Dias, Chammi S. P. G. *Angewandte Chemie International Edition* **2007**, *46*, 2192-2194.

(40) Omary, M. A.; Rawashdeh-Omary, M. A.; Diyabalanage, H. V. K.; Dias, H. V. R. *Inorganic Chemistry* **2003**, *42*, 8612-8614.

(41) Rasika Dias, H. V.; Polach, S. A.; Wang, Z. *Journal of Fluorine Chemistry* **2000**, *103*, 163-169.

(42) Dias, H. V. R.; Fianchini, M. *Comments on Inorganic Chemistry* **2007**, *28*, 73-92.

(43) Aiyea, E. C.; Ferguson, G.; AcAlees, A.; McCrindle, R.; Myers, R.; Siew, P. Y.; Dias, S. A. *J. Chem. Soc., Dalton Trans.* **1981**, 481.

(44) Dias, H. V.; Gamage, C. S. *Angew Chem Int Ed Engl* **2007**, *46*, 2192-4.

(45) Dias, H. V.; Wang, Z. *Inorg Chem* **2000**, *39*, 3890-3.

(46) Dias, H. V. R.; Singh, S.; Campana, C. F. *Inorganic Chemistry* **2008**, *47*, 3943-3945.

(47) Dias, H. V. R.; Wang, Z. *Inorganic Chemistry* **2000**, *39*, 3890-3893.

(48) Omary, M. A.; Mohamed, A. A.; Rawashdeh-Omary, M. A.; Fackler, J. J. P. *Coordination Chemistry Reviews* **2005**, *249*, 1372-1381.

(49) Burroughes, J . H.; Bradley, D. D. C.; Brown, A. R.; Marks, R. N.; Mackay, K.; Friend, R. H.; Burns, P. L.; Holmes, A. B. *Nature* **1990**, *v347*, p539(3).

(50) Wai-Yeung Wong, G.-J. Z. Z. H. K.-Y. C. A. M.-C. N. A. B. D.; cacute; Chan, W.-K. *Macromolecular Chemistry and Physics* **2008**, *209*, 1319-1332.

(51) Wolf, M. *Journal of Inorganic and Organometallic Polymers and Materials* **2006**, *16*, 189-199.

(52) Andrade, B. W. D.; Forrest, S. R. *Advanced Materials* **2004**, *16*, 1585-1595.

(53) Lamansky, S.; Djurovich, P.; Murphy, D.; Abdel-Razzaq, F.; Lee, H.-E.; Adachi, C.; Burrows, P. E.; Forrest, S. R.; Thompson, M. E. *Journal of the American Chemical Society* **2001**, *123*, 4304-4312.

(54) Namai, H.; Ikeda, H.; Hoshi, Y.; Kato, N.; Morishita, Y.; Mizuno, K. *Journal of the American Chemical Society* **2007**, *129*, 9032-9036.

(55) Furuta, P. T.; Deng, L.; Garon, S.; Thompson, M. E.; Frechet, J. M. J. *Journal of the American Chemical Society* **2004**, *126*, 15388-15389.

(56) Huang, Q.; Evmenenko, G.; Dutta, P.; Marks, T. J. *Journal of the American Chemical Society* **2003**, *125*, 14704-14705.

(57) Yuguang Ma, C.-M. C., Hsiu-Yi Chao, Xuemei Zhou, Wing-Han Chan, Jiaocong Shen, *Advanced Materials* **1999**, *11*, 852-857.

(58) Vaeth, K. M.; Tang, C. W. *Journal of Applied Physics* **2002**, *92*, 3447-3453.

(59) M. O. Wolf *Advanced Materials* **2001**, *13*, 545-553.

(60) Tong, C. C.; Hwang, K. C. *The Journal of Physical Chemistry C* **2007**, *111*, 3490-3494.

(61) Furuta, P.; Brooks, J.; Thompson, M. E.; Frechet, J. M. J. *Journal of the American Chemical Society* **2003**, *125*, 13165-13172.

(62) Cho, J.-Y.; Domercq, B.; Barlow, S.; Suponitsky, K. Y.; Li, J.; Timofeeva, T. V.; Jones, S. C.; Hayden, L. E.; Kimyonok, A.; South, C. R.; Weck, M.; Kippelen, B.; Marder, S. R. *Organometallics* **2007**, *26*, 4816-4829.

(63) Baldo, M. A.; O'Brien, D. F.; Thompson, M. E.; Forrest, S. R. *Physical Review B* **1999**, *60*, 14422.

(64) Yang, X.; Knobler, C. B.; Zheng, Z.; Hawthorne, M. F. *Journal of the American Chemical Society* **2002**, *116*, 7142-7159.

(65) Barron, J. A.; Bernhard, S.; Houston, P. L.; Abruna, H. D.; Ruglovsky, J. L.; Malliaras, G. G. *The Journal of Physical Chemistry A* **2003**, *107*, 8130-8133.

(66) Maness, K. M.; Masui, H.; Wightman, R. M.; Murray, R. W. *Journal of the American Chemical Society* **1997**, *119*, 3987-3993.

(67) Lee, J.-K.; Yoo, D.; Rubner, M. F. *Chemistry of Materials* **1997**, *9*, 1710-1712.

(68) S.-C. Lo; N.A.H. Male; J.P.J. Markham; S.W. Magennis; P.L. Burn; O.V. Salata; I.D.W. Samuel *Advanced Materials* **2002**, *14*, 975-979.

(69) Uson, R.; Laguna, A.; Garcia, J.; Laguna, M. *Inorganica Chimica Acta* **1979**, *37*, 201-207.

(70) Uson, R.; Laguna, A.; Brun, P. *Journal of Organometallic Chemistry* **1979**, *182*, 449-454.

(71) Uson, R.; Laguna, A.; Vicente, J. *Journal of Organometallic Chemistry* **1977**, *131*, 471-475.

(72) Usn, R.; Laguna, A.; Fernndez, E. J.; Mendia, A.; Jones, P. G. *Journal of Organometallic Chemistry* **1988**, *350*, 129-138.

(73) Fernandez, E. J.; Laguna, A.; Lopez-de-Luzuriaga, J. M.; Monge, M.; Montiel, M.; Olmos, M. E.; Perez, J.; Rodriguez-Castillo, M. *Gold Bull.* **2007**, *40*, 172-183.

(74) Mingos, D. M. P.; Crabtree, R. H. *Comprehensive organometallic chemistry III*; 1st ed.; Elsevier: Amsterdam ; Boston, 2007.

(75) Mingos, D. M. P.; John, Y.; Stephan, M.; David, J. W. *Angewandte Chemie International Edition in English* **1995**, *34*, 1894-1895.

(76) Dias, H. V.; Gamage, C. S.; Keltner, J.; Diyabalanage, H. V.; Omari, I.; Eyobo, Y.; Dias, N. R.; Roehr, N.; McKinney, L.; Poth, T. *Inorg Chem* **2007**, *46*, 2979-87.

(77) Dias, H. V.; Singh, S. *Inorg Chem* **2004**, *43*, 7396-402.

(78) Dias, H. V. R.; Fianchini, M. *Comments on Inorganic Chemistry* **2007**, *28*, 73-92.

(79) Dias, H. V. R.; Gamage, C. S. P.; Keltner, J.; Diyabalanage, H. V. K.; Omari, I.; Eyobo, Y.; Dias, N. R.; Roehr, N.; McKinney, L.; Poth, T. *Inorganic Chemistry* **2007**, *46*, 2979-2987.

(80) Omary, M. A.; Elbjeirami, O.; Gamage, C. S. P.; Sherman, K. M.; Dias, H. V. R. *Inorganic Chemistry* **2009**, *48*, 1784-1786.

(81) Morgan, H. H. *Journal of the Chemical Society* **1923**, *19*, 2901.

(82) Kubas, G. J. *Inorg. Synth.* **1979**, *19*, 90.

(83) G. J. Kubas, B. M., A. L. Crumblis, In *Inorganic Syntheses*; Robert, J. A., Ed. 2007, p 68-70.

(84) Omary, M. A.; Rawashdeh-Omary, M. A.; Diyabalanage, H. V. K.; Dias, H. V. R. *Inorganic Chemistry* **2003**, *42*, 8612-8614.